Published May 1, 1997

Intrinsic Voltage Dependence and Ca^{2+} Regulation of *mslo* Large Conductance Ca-activated K^+ Channels

J. Cui, D.H. Cox, and R.W. Aldrich

From the Department of Molecular and Cellular Physiology and Howard Hughes Medical Institute, Stanford University, Stanford, California 94305

ABSTRACT The kinetic and steady-state properties of macroscopic *mslo* Ca-activated K^+ currents were studied in excised patches from *Xenopus* oocytes. In response to voltage steps, the timecourse of both activation and deactivation, but for a brief delay in activation, could be approximated by a single exponential function over a wide range of voltages and internal Ca^{2+} concentrations ($[Ca]_i$). Activation rates increased with voltage and with $[Ca]_i$, and approached saturation at high $[Ca]_i$. Deactivation rates generally decreased with $[Ca]_i$ and voltage, and approached saturation at high $[Ca]_i$. Plots of the macroscopic conductance as a function of voltage (G-V) and the time constant of activation and deactivation shifted leftward along the voltage axis with increasing $[Ca]_i$. G-V relations could be approximated by a Boltzmann function with an equivalent gating charge which ranged between 1.1 and 1.8 *e* as $[Ca]_i$ varied between 0.84 and 1,000 μM. Hill analysis indicates that at least three Ca^{2+} binding sites can contribute to channel activation. Three lines of evidence indicate that there is at least one voltage-dependent unimolecular conformational change associated with *mslo* gating that is separate from Ca^{2+} binding. (*a*) The position of the *mslo* G-V relation does not vary logarithmically with $[Ca]_i$. (*b*) The macroscopic rate constant of activation approaches saturation at high $[Ca]_i$ but remains voltage dependent. (*c*) With strong depolarizations *mslo* currents can be nearly maximally activated without binding Ca^{2+}. These results can be understood in terms of a channel which must undergo a central voltage-dependent rate limiting conformational change in order to move from closed to open, with rapid Ca^{2+} binding to both open and closed states modulating this central step.

KEY WORDS: *mslo* • BK channel • voltage dependence • Ca^{2+} binding • gating

INTRODUCTION

Large conductance Ca-activated potassium channels (BK channels)[1] comprise a large group of membrane proteins found in a wide variety of cells (Latorre et al., 1989). These channels are identified by their potassium selectivity and large single channel conductance, as well as by their ability to sense changes in both membrane voltage and intracellular Ca^{2+} concentration (Lux et al., 1981; Marty, 1981; Pallotta et al., 1981; Barrett et al., 1982; Latorre et al., 1982; Latorre et al., 1989; Marty, 1989; McManus, 1991). When activated by an increase in intracellular Ca^{2+}, BK channels respond with increased open probability and concomitantly increased K^+ flux. These channels therefore can serve as a link between cellular processes which involve intracellular Ca^{2+} elevation and those which involve membrane excitability.

The proper functioning of BK channels depends not only on their ability to sense changes in membrane potential or intracellular Ca^{2+} concentration but also on the time course of their response. This is perhaps best exemplified in the inner hair cells of the turtle cochlea. Here, it has been demonstrated that there is a correlation between the frequency to which a particular hair cell is tuned and the kinetic properties of the BK channels native to that cell, suggesting that the kinetic behavior of these channels is critical for determining the frequency of the electrical oscillations in the hair cell during auditory stimulation (Hudspeth and Lewis, 1988*a*, *b*; Art et al., 1995; Wu et al., 1995).

Because the kinetic behavior of ion channels in general, and BK channels in particular, is critical for their proper function, and this behavior necessarily reflects the number and sequence of conformational states that a channel assumes as it gates, researchers have been interested in relating channel kinetics to the protein's underlying conformations. For BK channels this effort has been most successful at the single channel level where BK currents can be unambiguously identified and the internal Ca^{2+} concentration easily controlled. Extensive single channel studies on native BK channels have led to a kinetic picture in which there are at least five closed states and three open states with many paths between closed and open (McManus and Magleby, 1988; 1991). Hill analysis indicates that from two to perhaps as many as six Ca^{2+} ions can bind to the channel simultaneously, and it is likely that the different open states differ in the number of Ca^{2+} molecules bound (Barrett et al., 1982; Methfessel and Boheim, 1982; Moc-

Address correspondence to Dr. Richard W. Aldrich, Department of Molecular and Cellular Physiology, Beckman Center B171, Stanford, CA 94305-5426. Fax: 415-725-4463; E-mail: raldrich@popserver.stanford.edu

[1]*Abbreviation used in this paper:* BK channels, large conductance Ca-activated potassium channels.

Published May 1, 1997

zydlowski and Latorre, 1983; McManus et al., 1985; Golowasch et al., 1986; Oberhauser et al., 1988; McManus, 1991; McManus and Magleby, 1991; Art et al., 1995).

The voltage sensitivity of BK channel gating has been less extensively studied than its Ca^{2+} sensitivity. Single channel studies suggest, however, that the mechanism by which BK channels sense the membrane voltage may not be the same as that used by purely voltage-gated K^+ channels. In an extensive kinetic study, Moczydlowski and Latorre (1983) suggested that the voltage dependence of the gating properties of single skeletal muscle BK channels can be explained if it is supposed that the binding of Ca^{2+} to the channel is influenced by the transmembrane electric field, and it is this voltage sensitivity in Ca^{2+} binding that confers voltage-dependent gating properties on the channel rather than the action of voltage sensing elements intrinsic to the channel's primary sequence (see also Salomao et al., 1992). However, other studies have suggested, often on the basis of less extensive data and analysis, separate voltage-dependent and Ca-dependent steps in activation (Methfessel and Boheim, 1982; Blair and Dionne, 1985; Pallotta, 1985*b*; Cornejo et al., 1987; Singer and Walsh, 1987; Wei et al., 1994; DiChiara and Reinhart, 1995; Meera et al., 1996). Despite this previous work, the nature of the voltage-sensitive gating remains an open question.

The cloning of the pore forming subunits of several BK channels (Atkinson et al., 1991; Adelman et al., 1992; Butler et al., 1993; Tseng-Crank et al., 1994; McCobb et al., 1995; Wallner et al., 1995) has revealed some structural similarity between *slo* channels and *shaker*-type, purely voltage-gated K^+ channels. Although *slo* channels contain approximately twice as many amino acids as does a *shaker* channel, over the first ~330 amino acids of *slo* their predicted topologies are quite similar. *slo* channels contain a sequence homologous to the P region which forms a portion of the ion conducting pore and the selectivity filter of the *shaker* channel (MacKinnon and Yellen, 1990; Yellen et al., 1991; Yool and Schwarz, 1991; Heginbotham et al., 1992; 1994), as well as six (or seven, see Wallner et al., 1996) putative membrane spanning regions. The fourth such region (S4) contains several positively charged residues spaced in a similar manner as those found in the corresponding S4 region of voltage-gated ion channels. The S4 regions form, at least in part, the voltage sensing elements of these channels (Liman et al., 1991; Lopez et al., 1991; Papazian et al., 1991; Logothetis et al., 1993; Sigworth, 1994; Yang and Horn, 1995; Aggarwal and MacKinnon, 1996; Larsson et al., 1996; Mannuzzu et al., 1996; Seoh et al., 1996; Yang et al., 1996). The sequence of the remaining ~840 amino acids of *slo* channels appear to be unique to this channel family and is likely to contain Ca^{2+} binding domains (Lagrutta et al., 1994; Tseng-Crank et al., 1994; Wei et al., 1994).

The structural homology between cloned BK channels and voltage-gated K^+ channels is perhaps surprising given the lack of intrinsic voltage sensitivity suggested by previous single channel experiments (Moczydlowski and Latorre, 1983). It again raises the question as to whether the voltage-dependence of BK channel gating may be due at least in part to an intrinsic voltage sensing domain. Indeed the recent work of Wei et al. (1994) in which the COOH-terminal domain of *dslo* was combined with the NH_2-terminal domain of *mslo* suggests that this may be the case. Reports of voltage-dependent activation of BK channel currents at very low Ca^{2+} concentrations and after treatment to remove Ca^{2+} sensitivity suggest the possibility of an intrinsic voltage dependence as well (Barrett et al., 1982; Methfessel and Boheim, 1982; Wong et al., 1982; Findlay et al., 1985; Pallotta, 1985*b*; Meera et al., 1996).

To address this question, and to understand further the gating mechanisms of BK channels, we have taken advantage of the ability to express cloned channels at high density in *Xenopus* oocyte membranes to study the kinetic and steady-state properties of *mslo* macroscopic currents over a wide range of internal Ca^{2+} concentrations and membrane voltages. In this paper we present the basic steady-state and kinetic properties of these currents and discuss constraints these data place on any system designed to model the gating behavior of the *mslo* channel. A result of particular importance is that our data are not consistent with a model of *mslo* gating which ascribes the majority of the voltage dependence of activation to voltage-dependent Ca^{2+} binding; but rather, it is necessary to suppose that charges intrinsic to the channel protein are involved in voltage sensing. In fact, we find that with strong depolarizations it is possible to nearly maximally activate *mslo* channels at very low Ca^{2+} concentrations, so low as to not allow time for Ca^{2+} to bind to the channel before opening. Based on our analysis, a general scheme is proposed to account for the relationship between Ca-dependent and voltage-dependent activation of the *mslo* channel.

MATERIALS AND METHODS

Unless otherwise indicated, experiments were done using the conditions defined in the preceding paper (Cox et al., 1997). These conditions together with the appropriate analysis techniques allow for the discrimination between current properties arising from gating and those which are due to changes in channel permeation or block (Cox et al., 1997).

RESULTS

Voltage-dependent Properties of mslo Gating

One of the goals of this study is an extensive characterization of the macroscopic gating kinetics of *mslo* channels. Shown in Fig. 1 *A* is an experiment designed to ex-

Published May 1, 1997

amine the voltage dependence of *mslo* activation at a constant $[Ca]_i$. $[Ca]_i$ was buffered to 10.2 μM, and at 2-s intervals an excised membrane patch containing ~60 *mslo* channels was stepped from −100 mV to a series of increasingly more positive potentials. Several features of these currents are worth noting. First, at −100 mV the *mslo* channels were very seldom open as is indicated by the very low level of steady-state current. This was the case despite the presence of 10.2 μM Ca^{2+} in the solution exposed to the intracellular face of the patch, and thus demonstrates that, at this concentration, a negative membrane voltage can overcome any activating effects of Ca^{2+}. Second, upon depolarization, outward currents were observed which relaxed to their new steady-state level with a nearly single exponential time course. This can be seen most clearly in the middle panel in which a subset of traces have been expanded and fitted with exponential functions. There is some evidence, however, for a brief delay in the activation process. That is, when exponential fits such as those in Fig. 1 *A* are extrapolated backward in time to the point of zero current, they typically cross the time axis 75–175 μs after the beginning of the voltage step. After taking into account the appropriate filter delay (~33 μs, 4 pole bessel filter at 10 kHz), this result suggests an actual delay of 50–150 μs. Due to complications in directly observing the time course of ionic currents during the first ~100 μs after the voltage step, it is difficult to assess whether this apparent delay is an inherent property of the gating of *mslo* channels, or rather, at least in part an artifact produced by the subtraction of capacity and leak currents from the raw data before analysis. For this reason we have not emphasized this delay in our analysis and, in order to avoid errors, have fitted the time course of both activation and deactivation starting usually 200 μs after the beginning of the

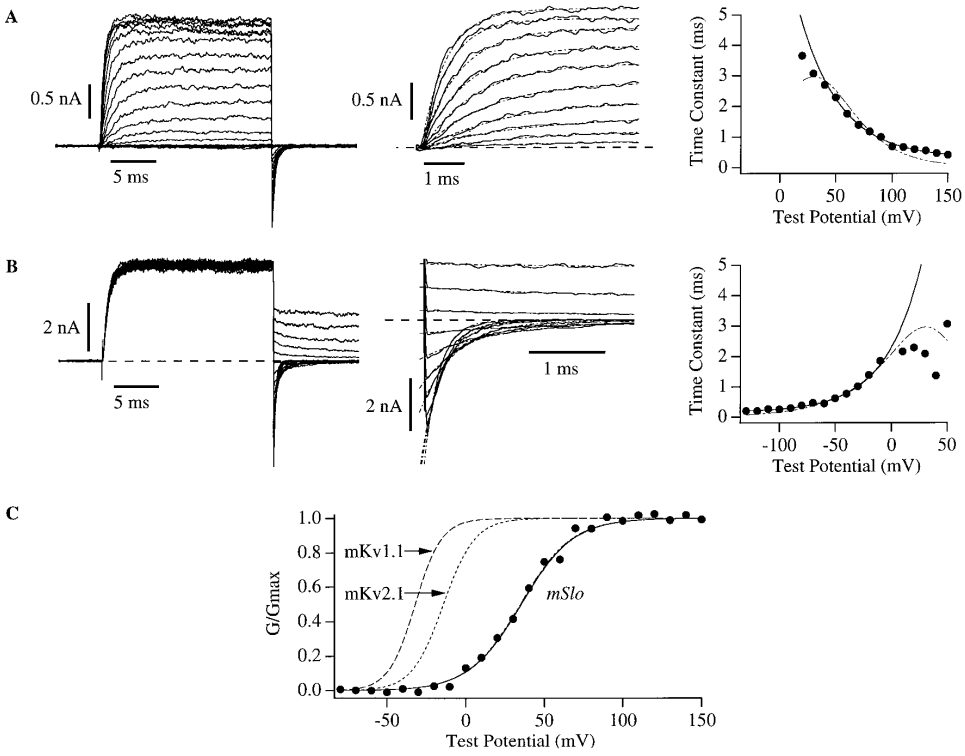

FIGURE 1. Macroscopic *mslo* K^+ currents recorded from inside out membrane patches during superfusion with 10.2 μM $[Ca]_i$. (*A*) (*left*) Current traces were elicited with 20-ms voltage steps to test potentials ranging from −80 to +150 mV in 10-mV increments. V_{hold} = −100 mV. After depolarization the membrane potential was repolarized to −80 mV. (*middle*) A subset of traces shown on the left have been expanded (+20 to +110 mV), and their activation time courses fitted with a single exponential function (*dashed lines*). (*right*) Plotted are the time constants of fits to the time course of activation as a function of test potential. Data points from +70 mV and more depolarized voltages were fitted with the function $\tau = Ae^{-qFV/RT} + b$ (*solid line*) with q = 0.71 and b = 0.31 ms. (*B*) (*left*) A family of tail current traces recorded in response to repolarizations to potentials ranging from −130 and +50 mV in 10 mV increments after 20 ms predepolarizations to +100 mV. (*middle*) A subset of traces from the left have been expanded (potentials −130 to +50 mV) and fitted with a single exponential function (*dashed lines*). (*right*) Time constants of fits to the time course of deactivation as a function of repolarization potential. Data points from −40 mV and more hyperpolarized voltages were fitted with the function $\tau = Ae^{qFV/RT} + b$ (*solid curve*) with q = 0.79 and b = 0.163. In *A* and *B* the currents displayed represent the averages of 4 and 2 families recorded in succession respectively. (*C*) Plotted is relative conductance (G/G_{max}) as a function of test potential for the data in *A*. Relative conductance was determined for each potential by measuring the tail current amplitude 200 μs after repolarization to −80 mV. The data were fitted (*solid curve*) with the Boltzmann function $G = G_{max}\{1/[1 + e^{-(V-V_{1/2})zF/RT}]\}$ with $V_{1/2}$ = +34.6 mV, z = 1.54 and then normalized to the maximum of the fit. Also included are the G-V relations for the mouse Kv1.1 and Kv2.1 K^+ channels. These curves were drawn according to published parameters for single Boltzmann fits (Kv1.1, Grissmer et al., 1994; Kv2.1, Pak et al., 1991). The broken curves in the right most panels of *A* and *B* represent fits to SCHEME I with $\alpha(V) = \alpha(0)e^{qFV/RT}$, $\alpha(0)$ = 53 s^{-1} qf = 0.86; $\beta(V) = \beta(0)e^{-qbFV/RT}$, $\beta(0)$ = 428 s^{-1}, qb = 0.68. In modeling the parameters were constrained so as to maintain the best fit to the G-V relation (*broken curve* superimposed on *solid curve* in *C*) The data in *A* and *B* are from separate patches. In this and subsequent figures dashed horizontal lines represent zero current.

Published May 1, 1997

voltage step. Preliminary experiments specifically designed to examine very early times in the activation process, however, suggest that this brief delay may truly reflect an aspect of the *mslo* gating process (see also Ottalia et al., 1996), and therefore further investigation is certainly warranted. And third, over the voltage range examined the time constant of *mslo* channel activation decreases with increasing voltage (Fig. 1 *A*, *right*).

The primarily exponential time course of activation suggests that, at 10.2 μM $[Ca]_i$, a single conformational change limits the rate at which *mslo* channels move from closed to open. The increasing rate of activation with increasing voltage could be explained if this conformational change were voltage dependent. To estimate the charge associated with this forward rate limiting transition we fitted the relationship between the time constant of activation and membrane voltage (Tau-V) with an exponential function. We limited the fit to depolarized voltages where reverse rates are likely to contribute less to the time course of activation. The fit superimposed on the data in Fig. 1 *A* (*right*) yielded a gating charge of 0.71 *e*. We found this estimate to be sensitive to the exact voltage range used and to whether or not the minimum of the exponential was allowed to vary. This estimate therefore is likely to represent only a rough approximation of the charge associated with this transition. From patch to patch, allowing the minimum to vary, this method yielded charge estimates ranging from 0.55 to 0.76 *e* (for mean see Table II). To obtain a lower limit for this number we fit the Tau-V curve over a wider voltage range, and fixed the minimum of the exponential to 0. Considering a single voltage-dependent rate limiting step in activation, at intermediate voltages where forward and backward rates become comparable, the contribution of the backward rate constant will be to decrease the observed activation time constant. This method is therefore likely to lead to an under estimate of the true charge. For the data in Fig. 1 *A*, fitting in this way produced an estimate of 0.47 charges (for mean see Table II).

Standard tail current protocols were used to study the voltage dependence of *mslo* deactivation. At 10.2 μM $[Ca]_i$ (Fig. 1 *B*), depolarizing voltage steps were applied to near maximally activate the channels, followed by hyperpolarizing steps to various potentials. Upon hyperpolarization, the channels closed, and the extent of tail current decay was voltage dependent. The time course of deactivation could be well approximated by a single exponential function over the entire voltage range examined (Fig. 1 *B*, *middle*), again suggesting a rate limiting conformational change between open and closed. The deactivation time constant was appreciably voltage dependent, increasing with depolarization. In Fig. 1 *B* (*right*), the time constant of deactivation, determined from exponential fits, is plotted as a function of membrane voltage. The charge associated with the apparent rate limiting backward transition in deactivation was estimated in a similar manner to that of activation. Exponential fits to the most hyperpolarized region of the Tau-V data (Fig. 1 *B*, *right*) yielded charge estimates ranging from 0.54 to 0.80 *e* (for mean see Table II). Fitting these Tau-V curves over a wider voltage range provided lower limit estimates of between 0.42 and 0.57 *e*.

Shown in Fig. 1 *C* is the conductance vs. voltage (G-V) relationship derived from the current traces in Fig. 1 *A*. The maximum slope of this relation, which is an indication of the voltage sensitivity of the channel, is less steep for *mslo* than for most purely voltage-gated K^+ channels suggesting that there may be comparatively less charge movement accompanying *mslo* gating. G-V curves for mouse Kv1.1(Grissmer et al., 1994) and Kv2.1(Pak et al., 1991) channels have been placed on Fig. 1 *C* for comparison. The *mslo* G-V curve has been fitted (*solid line*) with a Boltzmann function with an associated equivalent gating charge of 1.54 *e*, and a half activation voltage ($V_{1/2}$) of +34.6 mV. Notice that the equivalent gating charge associated with this fit (which represents a lower limit for the true gating charge of the channel) is approximately equal to the sum of the equivalent charges associated with forward and backward rate limiting kinetic transitions. Taking into account as well the monoexponential nature of current relaxations, these data point to a channel which, at 10.2 μM $[Ca]_i$, can be well approximated by a two-state system with similar voltage dependence in forward and backward transition rates:

$$C \underset{\beta(V)}{\overset{\alpha(V)}{\rightleftharpoons}} O. \qquad \text{(SCHEME I)}$$

Fits assuming such a model have been included in the Tau-V and G-V graphs of Fig. 1.

Ca^{2+}-dependent Properties of mslo Gating

To examine the Ca^{2+} dependence of *mslo* gating, we recorded macroscopic currents with protocols similar to that of Fig. 1 at a variety of $[Ca]_i$, from 0.84 to 1,000 μM (Figs. 2 and 3). In each experiment, as $[Ca]_i$ was increased it was necessary to hyperpolarize the holding voltage to maintain a low level of basal activity, as well as to adjust the range of the test voltages to accommodate the shifting activation range of the channels. What is perhaps most interesting in these data is that the essential characteristics of the *mslo* current traces recorded with 10.2 μM $[Ca]_i$ (Fig. 1) were maintained over the entire $[Ca]_i$ range tested. At each $[Ca]_i$ over the voltage range in which the time course of current relaxation could be accurately determined, the rate of activation increased with depolarization, and the rate

Published May 1, 1997

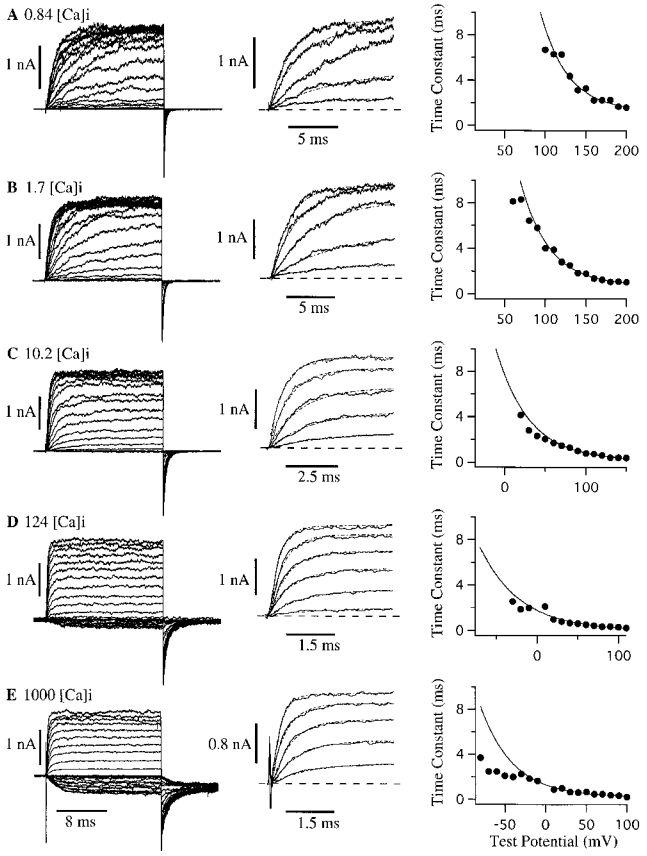

FIGURE 2. Activation of *mslo* currents. (*A–E*) Current traces from a single membrane patch recorded after a series of depolarizations to increasingly more positive membrane voltages. $[Ca]_i$ were as indicated (*top to bottom*) 0.84, 1.7, 10.2, 124, and 1,000 μM. Each series displayed is the average of 4 series recorded consecutively under identical conditions. Depolarizations were for 20 ms. Repolarizations were to −80 mV. In the left panels complete series are displayed. The voltage increment is 10 mV. In the middle panels a subset of traces have been expanded and fitted with single exponential functions (*dashed curves*). The voltage increment is 20 mV. In the right panels are shown plots of activation time constants as a function of test potential. The later portions of these curves are fitted with the function $\tau = Ae^{-qFV/RT} + b$ (*solid curves*). (*A*) 0.84 μM $[Ca]_i$, V_{hold} = −50 mV: (*left*) depolarizations ranged from 0 to +200 mV. (*middle*) Depolarizations ranged from +80 to +160 mV; (*right*) fit parameters: range +130 to 200 mV, $q = 0.77$, $b = 1.3$ ms. (*B*) 1.7 μM $[Ca]_i$, V_{hold} = −80 mV: (*left*) depolarizations ranged from −40 to +200 mV in 10-mV increments; (*middle*) depolarizations ranged from +60 to +140 mV; (*right*) fit parameters: range +120 to 200 mV, $q = 0.76$, $b = 0.76$ ms. (*C*) 10.2 μM $[Ca]_i$, V_{hold} = −100 mV: (*left*) depolarizations ranged from −80 to +150 mV; (*middle*) depolarizations ranged from +30 to +110 mV; (*right*) fit parameters: range +90 to +150 mV, $q = 0.63$, $b = 0.16$ ms (*D*) 124 μM $[Ca]_i$, V_{hold} = −120 mV: (*left*) depolarizations ranged from −120 to +110 mV; (*middle*) depolarizations ranged from +10 to +110 mV; (*right*) fit parameters: range −10 to +110 mV, $q = 0.52$, $b = 0.01$ ms. (*E*) 1,000 μM $[Ca]_i$, V_{hold} = −180 mV: (*left*) depolarizations ranged from −180 to +100 mV; (*middle*) depolarizations ranged from +20 to +100 mV; (*right*) fit parameters: range −10 to +100 mV $q = 0.64$, $b = 0.23$ ms.

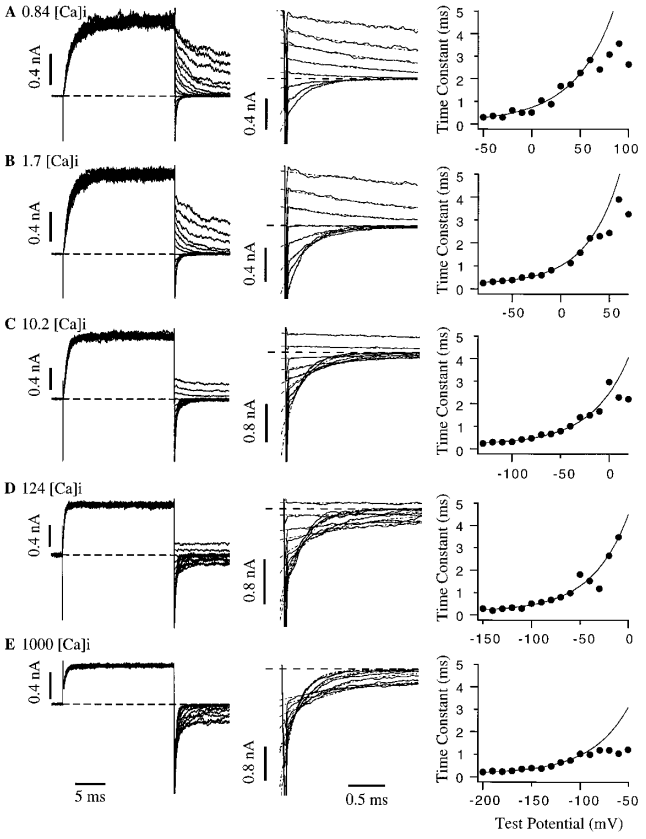

FIGURE 3. Deactivation of *mslo* currents. (*A–E*) Tail current families recorded from a single membrane patch. $[Ca]_i$ were as indicated (top to bottom): 0.84, 1.7, 10.2, 124, and 1,000 μM. Each family displayed is the average of 4 series recorded consecutively under identical conditions. Depolarizations are for 20 ms. Repolarizations are for 10 ms. In the left panels complete series are displayed. The voltage increment is 10 mV. In the middle panels subsets of traces from the left have been expanded and fitted with single exponential functions (*dashed curves*). The voltage increment is 20 mV. In the right panels are displayed plots of the deactivation time constant as a function of test potential. The most hyperpolarized portions of these curves are fitted with the function $\tau = Ae^{qFV/RT} + b$ (*solid curves*). (*A*) 0.84 μM $[Ca^{2+}]_i$: prepulse potential: 180 mV. Test potentials: −50 to 100 mV, $q = 0.62$, $b = 0.069$. (*B*) 1.7 μM $[Ca^{2+}]_i$: prepulse potential: 160 mV. Test potentials: −80 to 70 mV, $q = 0.74$, $b = 0.223$. (*C*) 10.2 μM $[Ca^{2+}]_i$: prepulse potential: 100 mV. Test potentials: −130 to 30 mV, $q = 0.67$, $b = 0.176$. (*D*) 124 μM $[Ca^{2+}]_i$: prepulse potential: 80 mV. Test potentials: −150 to 20 mV, $q = 0.68$, $b = 0.226$. (*E*) 1,000 μM $[Ca^{2+}]_i$: prepulse potential: 50 mV. Test potentials: −200 to −50 mV, $q = 0.67$, $b = 0.163$.

of deactivation generally decreased. Also, the kinetics of both activation and deactivation could be well fitted with single exponential functions (Figs. 2 and 3, *middle panels*), suggesting that the kinetics of activation and deactivation are dominated by a single conformational change. As was the case at 10.2 μM $[Ca]_i$, however, at each $[Ca]_i$ when exponential fits to the time course of activation were extrapolated to the point of zero current, they typically crossed the time axis between 50

Published May 1, 1997

and 150 μs after the onset of the voltage pulse, again suggesting the presence of a brief delay in the activation process.

Shown in the right panels of Figs. 2 and 3 are plots of the time constants of activation (Fig. 2) and deactivation (Fig. 3) as a function of voltage. The charges associated with the rate limiting transitions at each $[Ca]_i$ were estimated in the same manner as was done for the data in Fig. 1. As $[Ca]_i$ was varied the charge estimates associated with both forward and backward rate limiting transitions remained similar to that observed at 10.2 μM $[Ca]_i$. Although for activation there was a trend toward somewhat smaller charge estimates as $[Ca]_i$ was increased (see Table II), the predominant effect of raising $[Ca]_i$ was simply to translate the Tau-V curves of both activation and deactivation leftward along the voltage axis with little change in the voltage dependence of the kinetics (Fig. 4).

In addition to shifting the kinetics of *mslo* gating, raising $[Ca]_i$ caused a similar leftward shift in the G-V relationship. In Fig. 5 *A* is displayed a set of G-V curves recorded from a single membrane patch, and in Fig. 5 *B* are shown average G-V relations from several experiments. Curves corresponding to 0.84, 1.7, 4.5, 10.2, 65, 124, 490, and 1,000 μM $[Ca]_i$ are displayed. With both Tau-V curves (Fig 4) and G-V curves, for a given fold increase in $[Ca]_i$, we see a larger shift at low $[Ca]_i$ (e.g., between 0.84 and 10.2 μM) than at higher $[Ca]_i$ (e.g., between 124 and 1,000 μM). As will be discussed later, this property with regard to the Ca^{2+} dependence of the G-V relation is in agreement with previously published data (Wei et al., 1994) and has important implications for the physical relationship between Ca^{2+} binding and voltage sensing. As $[Ca]_i$ was varied, the G-V relation maintained a shape which could be approximated by a single Boltzmann function, and the slope of this relation was similar at each $[Ca]_i$ (Table I). That is, as with the kinetics of activation and deactivation, the predominant effect of an increase in $[Ca]_i$ was to simply translate the G-V curve leftward along the voltage axis. Similar data have been published for both native (Barrett et al., 1982; Latorre et al., 1982; Methfessel and Boheim, 1982; Moczydlowski and Latorre, 1983; Markwardt and Isenberg, 1992; Art et al., 1995; Giangiacomo et al., 1995) and cloned (Butler et al., 1993; Tseng-Crank et al., 1994; Wei et al., 1994; DiChiara and Reinhart, 1995; McCobb et al., 1995; McManus et al., 1995; Wallner et al., 1995; Meera et al., 1996) BK channels.

We did, however, see some change in the slope factor of fits to the *mslo* G-V relation as $[Ca]_i$ was varied. In particular there was a trend toward shallower slopes as $[Ca]_i$ was increased above 1.7 μM. In Fig. 5 *A*, for example, equivalent gating charge estimates as determined from Boltzmann fits varied between extremes of 1.88, at 1.7 μM $[Ca]_i$, to 1.18 at 1,000 μM $[Ca]_i$. This is representative of the behavior observed in several experiments (see Table I and Fig. 5 *B*) and is therefore not due to random variability in the data. As discussed in the preceding paper (Cox et al., 1997), contaminant Ba^{2+} block at high voltages might cause a small increase in the steepness of the G-V curve measured at 0.84 μM $[Ca]_i$. At 1.7 μM $[Ca]_i$ and above, however, the G-V curve spans less depolarized voltages, and Ba^{2+} block is not likely to have a significant effect (Cox et al. 1997). Therefore, this trend may reflect a genuine change in

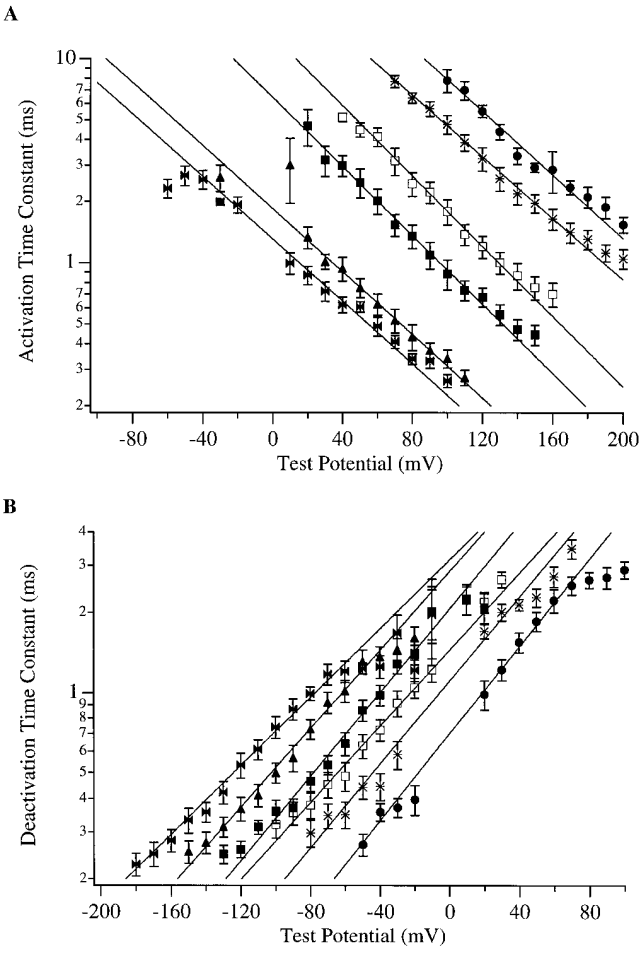

FIGURE 4. Mean activation and deactivation time constant as a function of both voltage and $[Ca]_i$. Displayed are semi-log plots of activation (*A*) and deactivation (*B*) time constants. Each curve represents the mean of between 4 and 10 experiments. Error bars indicate standard errors of the mean. Solid lines represent fits to the function $\tau = Ae^{-qFV/RT}$. Fits were done by eye. Fit parameters: (*A*) $[Ca]_i$ = 0.84 μM (●), $n = 4$, $q = 0.46$; $[Ca]_i$ = 1.7 μM (*), $n = 10$, $q = 0.44$; $[Ca]_i$ = 4.5 μM (□), $n = 9$, $q = 0.51$; $[Ca]_i$ = 10.2 μM (■), $n = 7$, $q = 0.50$; $[Ca]_i$ = 124 μM (▲), $n = 7$, $q = 0.45$; $[Ca]_i$ = 1,000 μM (▶◀), $n = 5$, $q = 0.45$. (*B*) $[Ca]_i$ = 0.84 μM (●), $n = 7$, $q = -0.48$; $[Ca]_i$ = 1.7 μM (*), $n = 6$, $q = -0.46$; $[Ca]_i$ = 4.5 μM (□), $n = 7$, $q = -0.42$; $[Ca]_i$ = 10.2 μM (■), $n = 10$, $q = -0.46$; $[Ca]_i$ = 124 μM (▲), $n = 9$, $q = -0.43$; $[Ca]_i$ = 1,000 μM (▶◀), $n = 10$, $q = -0.38$.

Published May 1, 1997

TABLE I

Steady-state G-V Parameters

	$G/G_{max} = 1/(1+e^{zF(V_{1/2}-V)/RT})$	
$[Ca]_i$ (μM)	$V_{1/2}$ (mV)	z
0.84	112 ± 3.8* (11)‡	1.62 ± 0.066*
1.7	84.6 ± 3.7 (13)	1.79 ± 0.057
4.5	53.0 ± 4.3 (11)	1.62 ± 0.079
10.2	29.9 ± 3.1 (16)	1.46 ± 0.056
65	−0.1 ± 3.2 (10)	1.30 ± 0.042
124	−8.3 ± 2.9 (15)	1.32 ± 0.034
490	−22.7 ± 4.0 (14)	1.19 ± 0.047
1000	−34.6 ± 2.9 (13)	1.15 ± 0.047

*Values are given as mean ± standard error. ‡In parentheses is the number of experiments used to determine each value.

the voltage dependence of *mslo* gating as $[Ca]_i$ is increased.

The effects of varying $[Ca]_i$ are more easily seen when a single voltage is considered (Fig. 6). In Fig. 6 *A* are shown several traces recorded in response to voltage steps to +70 mV. Traces labeled *a* through *f* were recorded at increasing $[Ca]_i$ (see legend). Several features of these currents are apparent. First, as expected for a Ca-activated channel, peak current amplitude increased with $[Ca]_i$. This point is only strictly true for the traces recorded in the $[Ca]_i$ range 0.84–124 μM. At higher $[Ca]_i$, peak current actually declined. This decline, however, became more pronounced as $[Ca]_i$ was increased and was not associated with a decline in tail current amplitude at −80 mV. It can therefore be attributed to voltage-dependent Ca^{2+} block (see preceding paper in this issue, Cox et al., 1997) and as such is not indicative of an actual reduction in channel activity. Second, as can be seen when the currents in *A* are normalized to their maxima (Fig. 6 *B*), the rate of current activation increased with increasing $[Ca]_i$, while the rate of deactivation decreased (Fig. 6 *C*). And third, as emphasized by the exponential fits superimposed on the traces in *B* and *C*, the primarily monoexponential nature of both activation and deactivation was maintained as $[Ca]_i$ was varied.

Plotted in Fig. 6 *D* is the relationship between relative conductance and $[Ca]_i$ at +70 mV. This relation was determined from the G-V curves of Fig. 5, amounting

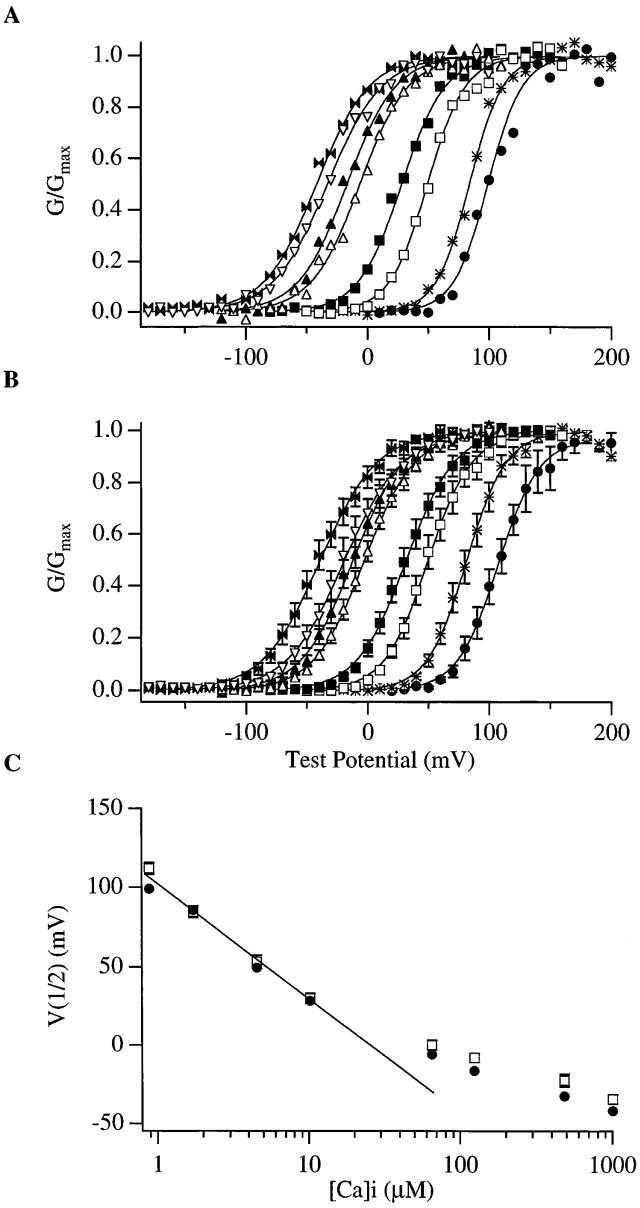

of the fit. Curves plotted with filled symbols represent approximately 10-fold increases in $[Ca]_i$, as do curves plotted with open symbols. (*C*) Plot of the voltage at half maximal activation $V_{1/2}$ vs. $[Ca]_i$ as determined from fits to the data in *A* (●). Also plotted are the mean $V_{1/2}$ values from several individual experiments (□). Error bars represent standard error of the mean with n = 11, 13, 11, 16, 10, 15 14, 13 for $[Ca]_i$ = 0.84, 1.7, 4.6, 10.2, 65, 124, 490, 1,000 μM, respectively. In *A* and *B* the parameters of the fits were as follows: (*A*) $[Ca]_i$ = 0.84 μM, $V_{1/2}$ = 99.0 mV, z = 1.8; $[Ca]_i$ = 1.7 μM, $V_{1/2}$ = 85.6 mV, z = 1.88; $[Ca]_i$ = 4.6 μM, $V_{1/2}$ = 49.4 mV, z = 1.62; $[Ca]_i$ = 10.2 μM, $V_{1/2}$ = 28.2 mV, z = 1.44; $[Ca]_i$ = 65 μM, $V_{1/2}$ = −6.2 mV, z = 1.27; $[Ca]_i$ = 124 μM, $V_{1/2}$ = −16.7 mV, z = 1.27; $[Ca]_i$ = 490 μM, $V_{1/2}$ = −32.7, z = 1.13; $[Ca]_i$ = 1,000 μM, $V_{1/2}$ = −41.8 mV, z = 1.18. (*B*) $[Ca]_i$ = 0.84 μM, $V_{1/2}$ = 107 mV, z = 1.52, n = 5; $[Ca]_i$ = 1.7 μM, $V_{1/2}$ = 81.5 mV, z = 1.56, n = 10; $[Ca]_i$ = 4.6 μM, $V_{1/2}$ = 49.6 mV, z = 1.44, n = 9; $[Ca]_i$ = 10.2 μM, $V_{1/2}$ = 32.0 mV, z = 1.27, n = 7; $[Ca]_i$ = 65 μM, $V_{1/2}$ = −2.7 mV, z = 1.24, n = 8; $[Ca]_i$ = 124 μM, $V_{1/2}$ = −11.8 mV, z = 1.20, n = 7; $[Ca]_i$ = 490 μM, $V_{1/2}$ = −19.4, z = 1.09, n = 8; $[Ca]_i$ = 1,000 μM, $V_{1/2}$ = −38.9 mV, z = 1.08, n = 5.

FIGURE 5. Normalized conductance vs. voltage relations from a single membrane patch (*A*) and the average of several patches (*B*) are displayed for the following $[Ca]_i$: 0.84 (●), 1.7 (*), 4.6 (□), 10.2 (■), 65 (△), 124 (▲), 490 (▽), 1,000 μM (▶◀). Relative conductance was determined for each test potential by measuring the tail current amplitude 200 μs after repolarization to −80 mV. The data were fitted (*solid curve*) with the Boltzmann function $G = G_{max}(1/(1+e^{-(V-V_{1/2})zF/RT}))$ and then normalized to the maximum

Published May 1, 1997

essentially to a transformation of these data to $[Ca]_i$ dose response form. As was the case for the G-V relations, G/G_{max} plotted on the ordinate is proportional to open probability. The smooth curve through the data represents a fit to the Hill equation below (Hill, 1910).

$$G/G_{max} = A\left[\frac{1}{1+\left(\frac{K_D}{[Ca]_i}\right)^n}\right]. \quad (1)$$

Here K_D represents the apparent Ca^{2+} dissociation constant, n the Hill coefficient, and A the maximum value of G/G_{max}. The Hill coefficient ($n = 3.08$) from this fit is within the range of values reported in studies of single BK channel gating (Barrett et al., 1982; Moczydlowski and Latorre, 1983; Golowasch et al., 1986; Oberhauser et al., 1988; McManus and Magleby, 1991). The fact that this value is greater than 1 indicates that more than one Ca^{2+} molecule binds to the *mslo* channel, and that Ca^{2+} binds in a cooperative manner (Adair, 1925). The apparent K_D determined from the fit is 1.44 μM.

Plotted in Fig. 6 *E* is the relationship between the macroscopic rate constant of *mslo* current activation (the reciprocal of the time constant) and $[Ca]_i$ also at +70 mV. There is not a linear relationship between these variables as would be expected from a system whose macroscopic rate constant was limited by a Ca^{2+} binding transition. The data are better described by a hyperbolic function which approaches a saturating value at high $[Ca]_i$. This result indicates that changes in the rate constants of kinetic transitions which involve Ca^{2+} binding no longer affect the kinetic behavior of the system at high $[Ca]_i$. This saturating behavior cannot be explained by kinetic schemes which involve only Ca^{2+} binding steps. Considering, for example, a scheme composed of a string of n Ca^{2+} binding steps:

$$C_1 \underset{k_{-1}}{\overset{k_1[Ca]}{\rightleftharpoons}} C_2 \underset{k_{-2}}{\overset{k_2[Ca]}{\rightleftharpoons}} \ldots \underset{k_{-(n-1)}}{\overset{k_{(n-1)}[Ca]}{\rightleftharpoons}} O_n. \quad \text{(SCHEME II)}$$

the activation time course for SCHEME II will contain $(n-1)$ exponential components. As $[Ca]_i$ is increased, the forward rates become much larger than the backward rates, and each of the macroscopic rate constants of the system approaches one of the first order forward rate constants. Thus, at high $[Ca]_i$, each of the macroscopic rate constants (r_i) becomes a linear function of $[Ca]_i$.

$$r_i = k_i[Ca], \quad \text{for } i = \{1, 2, 3 \ldots . (n-1)\}. \quad (2)$$

To account for the saturating behavior in Fig. 6 *E* then, there must be at least one elementary step in the gating of the *mslo* channel which does not involve Ca^{2+} binding and serves to limit the rate of activation at high

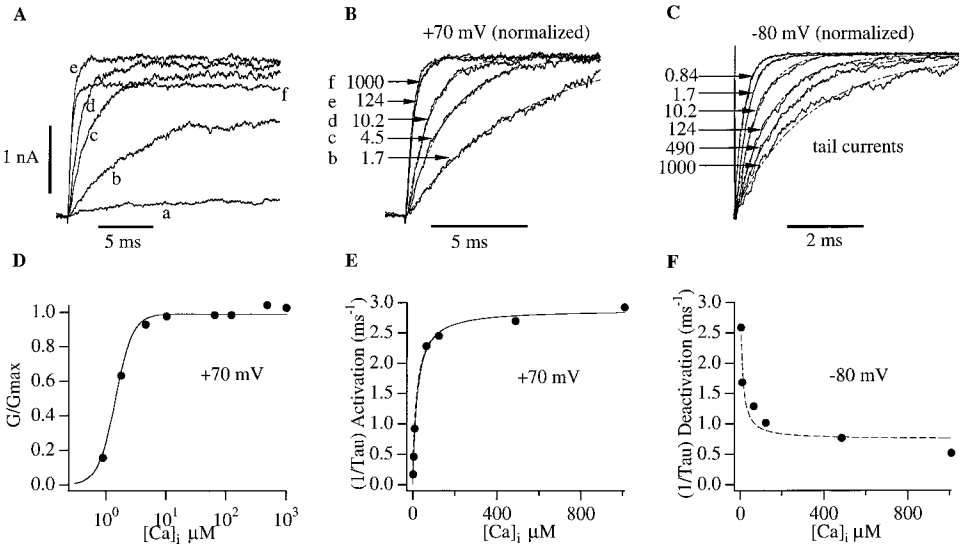

FIGURE 6. Ca dependence of *mslo* currents. (*A*) Current traces recorded during 20-ms depolarizations to +70 mV at a series of $[Ca]_i$. $[Ca]_i$ are, in alphabetical order: 0.84, 1.7, 4.5, 10.2, 124, 1,000 μM. In (*B*) several of the currents from *A* have been normalized to their maximum and superimposed for comparison. Also displayed are single exponential fits to the time course of activation (*dashed lines*). (*C*) Tail currents were recorded at −80 mV after 20-ms voltage steps to +100 mV. These currents were then normalized to their minimums and superimposed. $[Ca]_i$ are as indicated. Also displayed are single exponential fits to the time course of deactivation (*dashed lines*). In (*D*) the fraction of channels activated in *A* is plotted as a function of $[Ca]_i$. Normalized conductances (G/G_{max}) were derived from conductance-voltage relations determined at each $[Ca]_i$ from tail current measurements as described for Fig. 5. The data are fitted (*solid curve*) to the equation: $G/G_{max} = Amp(1/\{1+(K_D/[Ca])^n\})$ with the following parameters ($Amp = 0.99$, $K_D = 1.44$ μM, $n = 3.08$). In *E* and *F* the macroscopic rate constants for current activation *E* and deactivation *F*, as determined from single exponential fits, are plotted as a function of $[Ca]_i$. In *E* the data are fitted with two functions. The solid curve represents a fit to Eq. 3 with $\alpha = 2.88$ ms^{-1}, $k_{-1}/k_1 = 20.8$ μM, and $\beta = 0$. The dashed curve represents a fit to Eq. 4 with $\alpha = 2.89$ ms^{-1}, $k_{-1}/k_1 = 20$ μM, $\beta = 0.3$, and $k_{-3}/k_3 = 10$ μM. In *F* the data are fitted with Eq. 4 with $\alpha = 0.74$ ms^{-1}, $k_{-1}/k_1 = 20$ μM, $\beta = 3.40$, and $k_{-3}/k_3 = 10$ μM.

Published May 1, 1997

$[Ca]_i$. The minimum scheme contains one Ca^{2+} binding step and one Ca-independent step (SCHEME III below).

$$C_0 \underset{k_{-1}}{\overset{k_1[Ca]}{\rightleftharpoons}} C_1 \underset{\beta}{\overset{\alpha}{\rightleftharpoons}} O_2. \qquad \text{(SCHEME III)}$$

In general, a three-state kinetic scheme like SCHEME III will have a relaxation time course described by the sum of two exponential functions. This is contrary to the monoexponential nature of the *mslo* currents. The kinetic behavior of SCHEME III, however, will be dominated by a single exponential component if the rate constants for one step are fast relative to those for the other step. For *mslo* it would have to be the Ca^{2+} binding step which equilibrates most rapidly; otherwise, the activation rate could not become Ca-independent at high $[Ca]_i$. Making this designation then, the dominant macroscopic rate constant r for SCHEME III becomes:

$$r \cong \alpha\left[\frac{1}{1+\frac{k_{-1}}{k_1[Ca]}}\right] + \beta. \qquad (3)$$

This function is the rectangular hyperbola used to fit the data in Fig. 6 *E* (*solid line*), thus demonstrating that by including a Ca-independent step a very simple system can account for the saturating behavior of the macroscopic rate constant of activation at high $[Ca]_i$.

SCHEME III, however, is not sufficient to account simultaneously for the Ca^{2+} dependence of the macroscopic rate constant of activation at +70 mV and the macroscopic rate constant of deactivation at −80 mV (Fig. 6 *F*). As with activation, the kinetics of deactivation become much less Ca^{2+} sensitive at high $[Ca]_i$. At lower concentrations, however, deactivation kinetics are slowed rather than accelerated as $[Ca]_i$ is increased. This behavior cannot be explained by SCHEME III because, according to Eq. 3, under no condition will the relaxation rate of this system decrease as $[Ca]_i$ is increased. To account for the Ca^{2+} dependence of both activation and deactivation kinetics it is necessary to add another Ca-dependent step to SCHEME III.

$$\begin{array}{ccc} C_0 & \underset{k_{-1}}{\overset{k_1[Ca]}{\rightleftharpoons}} & C_1 \\ & \beta \uparrow\downarrow \alpha & \\ O_2 & \underset{k_{-3}}{\overset{k_3[Ca]}{\rightleftharpoons}} & O_3. \end{array} \qquad \text{(SCHEME IV)}$$

If a Ca^{2+} binding step is added after opening (SCHEME IV), again assigning rapid Ca^{2+} binding on and off rates to maintain exponential kinetics, the macroscopic rate constant for SCHEME IV is approximated by:

$$r \cong \alpha\left[\frac{1}{1+\frac{k_{-1}}{k_1[Ca]}}\right] + \beta\left[1-\frac{1}{1+\frac{k_{-3}}{k_3[Ca]}}\right]. \qquad (4)$$

This equation contains two terms, one containing α weighted by the fraction of closed channels in C_1 which increases with increasing $[Ca]_i$ and the other containing β weighted by the fraction of open channels in O_2 which decreases with increasing $[Ca]_i$. Whether the macroscopic rate constant of this system increases or decreases as $[Ca]_i$ is increased will depend upon which term is changing more rapidly. In general, depending on the specific binding and unbinding rates, when α is greater than β, the first term will increase more rapidly than the second term decreases, and the macroscopic relaxation rate constant of the system will increase with increasing $[Ca]_i$. Conversely, when β is greater than α, the second term will change more rapidly than the first, and the macroscopic relaxation rate constant will decrease as $[Ca]_i$ is increased. In either case, at high $[Ca]_i$, saturation is expected with r_{sat} equal to α. Therefore, if the rate constants α and β were to change with voltage, SCHEME IV could qualitatively explain both the increasing rate of *mslo* current activation as a function of $[Ca]_i$ at +70 mV and the decreasing rate of deactivation as a function of $[Ca]_i$ at −80 mV. The data in Fig. 6 *E* and *F* have been fitted with Eq. 4 (*dashed lines*) simply by changing the values of α and β.

Another observation we might make with regard to the data in Fig. 6 is that at +70 mV it takes less Ca^{2+} to saturate the channel's steady-state conductance G/G_{max} (which is proportional to open probability) than it does to saturate the macroscopic rate constant of activation. Can we understand this behavior in terms of SCHEME IV as well? To answer this question it is useful to write the open probability of SCHEME IV as:

$$P_{open} = \frac{\alpha\left[\frac{1}{1+\frac{k_{-1}}{k_1[Ca]}}\right]}{\alpha\left[\frac{1}{1+\frac{k_{-1}}{k_1[Ca]}}\right] + \beta\left[1-\frac{1}{1+\frac{k_{-3}}{k_3[Ca]}}\right]}, \qquad (5)$$

and compare it to the expression for the relaxation rate constant, Eq. 4. The differences between these expressions are that the terms involving α and β in Eq. 4 are now in the denominator of Eq. 5, and the term containing α is in the numerator. This term represents α weighted by the fraction of channels occupying state C_1

Published May 1, 1997

at equilibrium. Supposing that α and β are voltage-dependent and that α is several fold larger than β at +70 mV, it will then not be necessary for the closed state Ca^{2+} binding step to be saturated for the channel to be very nearly maximally activated. It is necessary only that $\alpha\{1/(1 + k_{-1}/k_1[Ca])\}$, which increases with $[Ca]_i$, be much larger than $\beta(1 - \{1/(1 + k_{-3}/k_3[Ca])\})$, which decreases with $[Ca]_i$. As is evident from Eq. 4, however, in order for the kinetic behavior of the system to be saturated, the closed state binding step must be fully saturated, and therefore $[Ca]_i$ must be severalfold greater than K_{D1} (k_{-1}/k_1). Thus it is clear that, given a wide rage of parameters, SCHEME IV predicts another aspect of the data: the apparent K_D estimated from steady-state conductance measurements might be considerably smaller than that estimated from kinetic measurements.

mslo Gating Involves Voltage-dependent Steps which Are Distinct from Ca^{2+} Binding Steps

The preceding analysis illustrates that many aspects of *mslo* gating can be understood, at least qualitatively, in terms of a central closed to open, voltage-dependent, conformational change flanked by rapid Ca^{2+} binding steps. In fact, Methfessel and Boheim (1982) have proposed a model which takes the form of SCHEME IV to account for the Ca-dependent and voltage-dependent gating properties of single skeletal muscle BK channels. Moczydlowski and Latorre (1983), however, were able to account for many properties of those same channels by considering a scheme identical to SCHEME IV excepting that all of the voltage dependence of the system resided in the voltage dependence of Ca^{2+} binding. Models based on their idea can successfully predict several features of our data: (*1*) approximately exponential kinetic behavior, (*b*) a G-V relation which can be approximated by a Boltzmann function at any $[Ca]_i$, (*c*) channels which can be both maximally activated and deactivated at any nonzero $[Ca]_i$, and (*d*) a leftward shift in the G-V curve when $[Ca]_i$ is increased. However, as also shown by Wei et al. (1994) such a gating mechanism can be tentatively excluded for *mslo* based on the observation that for each 10-fold increase in $[Ca]_i$ the channel's G-V curves are not evenly spaced (Fig. 5, see also DiChiara and Reinhart, 1995).

To see that this is the case, it is useful to first consider the simplest form of a voltage-dependent binding mechanism in which there is a single Ca^{2+} binding site some distance into the plasma membrane such that in binding, Ca^{2+} traverses a fraction of the membrane voltage δ (the electrical distance). In this case the probability of the binding site being occupied by Ca^{2+}, and thus the channel being open (P_o), depends on $[Ca]_i$ as follows (Woodhull, 1973).

$$P_o = \frac{1}{1 + \frac{K_D(0)\, e^{-\frac{2\delta FV}{RT}}}{[Ca]_i}}, \quad (6)$$

where F represents Faraday's constant, R the universal gas constant, T temperature, and $K_D(0)$ the Ca^{2+} dissociation constant at 0 mV. Analyzing Eq. 6 in terms of the voltage required to reach half maximal activation ($V_{1/2}$), we see that for P_o equal to 0.5, we must have

$$\frac{K_D(0)}{[Ca]_i} e^{-\frac{2\delta FV_{1/2}}{RT}} = 1. \quad (7)$$

This equation can be rewritten as

$$V_{1/2} = -\frac{2.303RT}{2\delta F}\log([Ca]_i) + \frac{2.303RT}{2\delta F}\log[K_D(0)], \quad (8)$$

(Wong et al., 1982) which predicts a logarithmic relationship between $V_{1/2}$ and $[Ca]_i$.

Plotted in Fig. 5 C is the relationship between $V_{1/2}$ and $[Ca]_i$ for the data in Fig. 5 A (*closed circles*). Also shown are the average $V_{1/2}$ values from several experiments (*open squares*). The curvature in these plots is indicative of the closer spacing of the G-V curves at higher $[Ca]_i$. This behavior was seen in every experiment in which G-V curves where determined at 3 or more $[Ca]_i$ ($n = 13$). In the experiment of Fig. 5 *A* Ca^{2+} was presented to the patch in the following order: 1.7, 4.5, 65, 490, 124, 10.2, 0.84, and 1,000 μM, thus ruling out the possibility that the tendency toward closer G-V spacing at high $[Ca]_i$ was due to a slow, time-dependent change in *mslo* current properties. From the curvature in the plot of Fig. 5 *C* then, we can rule out the single voltage-dependent Ca^{2+} binding site model. However, *mslo* is thought to be a tetramer (Shen et al., 1994), and is likely to have more than one Ca^{2+} binding site (Fig. 6 *D*). Nevertheless, it turns out that for a large class of models with multiple binding sites a logarithmic relationship between $V_{1/2}$ and $[Ca]_i$ is predicted. The following statement holds true: For models of channel gating in which the voltage dependence of gating resides solely in the voltage dependence of Ca^{2+} binding, regardless of the number of Ca^{2+} binding sites or their affinities for Ca^{2+}, there will be a logarithmic relationship between $V_{1/2}$ and $[Ca]_i$ so long as the electrical distances of all the binding sites are equivalent. A conclusion very similar to this was arrived at by Wei et al. (1994) through simulations of various possible gating schemes. Below we provide a mathematical argument which extends their analysis.

In a channel with multiple binding sites, whose occupancy somehow relates to channel opening, the probability of a given site being occupied by Ca^{2+} at any given

Published May 1, 1997

time will depend on the Ca^{2+} concentration and the affinity of each site, such that the overall probability of the channel being open is a function of all of the dissociation constants:

$$P_o = f\left(\frac{[Ca]_i}{K_1}, \frac{[Ca]_i}{K_2}, \ldots, \frac{[Ca]_i}{K_n}, C\right), \quad (9)$$

where K_1 through K_n represent the Ca^{2+} dissociation constants of binding sites 1 through n, and C represents the combined effects of all elementary steps not involving Ca^{2+} binding. If Ca^{2+} binding is voltage dependent, then each dissociation constant can be written as

$$K_j(V) = K_j(0)\, e^{-\frac{2\delta_j FV}{RT}}, \quad (10)$$

where j ranges from 1 to n, $K_j(0)$ represents the Ca^{2+} dissociation constant of the jth site at 0 mV, and δ_j represents the electrical distance of the jth site. From Eq. 10 we may write for each binding site in Eq. 9:

$$\frac{[Ca]_i}{K_j} = \frac{[Ca]_i}{K_j(0)} e^{\frac{2F\delta_j V}{RT}} = \frac{C^o}{K_j(0)} e^{\frac{2F\delta_j (V - X_j)}{RT}}, \quad (11)$$

with

$$[Ca]_i = e^{\frac{-2F\delta_j X_j}{RT}} C^o, \quad (12)$$

where

$$C^o \equiv 1 \text{ mol/liter},$$

or conversely,

$$X_j = -\frac{RT}{2\delta_j F} \ln\left[\frac{[Ca]_i}{C^o}\right]. \quad (13)$$

From Eqs. 11, 12, and 13, we see that X_j varies logarithmically with $[Ca]_i$, and that in order to maintain $(V - X_j)$ constant in Eq. 11, and therefore $[Ca]/K_j$ constant as well, the necessary change in membrane voltage will be equal to the change in X_j. That is,

$$\Delta V = \Delta X_j = -\frac{RT}{2\delta_j F} \Delta \ln\left[\frac{[Ca]_i}{C^o}\right]. \quad (14)$$

If we suppose, as stipulated above, that all Ca^{2+} binding sites have the same voltage dependence,

$$\delta_j = \delta, \text{ for } j = \{1, 2, ..., n\}, \quad (15)$$

then as [Ca] is varied the change in voltage necessary to maintain $[Ca]/K_j$ constant is the same at each binding site and given as

$$\Delta V = -\frac{RT}{2\delta F} \Delta \ln\left[\frac{[Ca]_i}{C^o}\right]. \quad (16)$$

Because we are considering cases in which all of the channel's voltage dependence resides in Ca^{2+} binding steps, the change in P_o in response to a change in voltage is determined solely by the effects of voltage on the Ca^{2+} binding equilibria (i.e., C in Eq. 9 is independent of voltage), and therefore the change in voltage necessary to maintain P_o constant as $[Ca]_i$ is varied is also given by Eq. 16. A logarithmic relationship is therefore expected between a change in $[Ca]_i$ and the change in voltage necessary to maintain any specific P_o. Choosing P_o equal to 0.5 as a convenient reference, the voltage necessary to maintain $P_o = 0.5$ is explicitly given as the following function of [Ca]:

$$V_{1/2} = -\frac{2.303RT}{2\delta F} \log\left[\frac{[Ca]_i}{C^o}\right] + \frac{2.303RT}{2\delta F} \log\left[\frac{[Ca]_{1/2}}{C^o}\right]. \quad (17)$$

Here $[Ca]_{1/2}$ is defined as the concentration of Ca^{2+} necessary to half maximally activate the channels at 0 mV.

Thus, we can say that the data in Fig. 5 are inconsistent with gating models in which the voltage dependence lies solely in Ca^{2+} binding to binding sites having equivalent electrical distances. When the electrical distances are not the same, the effect of voltage is different at each site and the situation is more complex. Two aspects of our data, however, suggest that if the voltage dependence of *mslo* gating were to arise solely from voltage-dependent Ca^{2+} binding, then the electrical distances for the *mslo* Ca^{2+} binding sites would have to be similar. The first is that computer simulations of models involving multiple voltage-dependent Ca^{2+} binding sites indicate that as the δ values for the sites diverge, the predicted G-V relation deviates markedly from Boltzmann behavior at either low or high $[Ca]_i$. No such effect is seen in the *mslo* data. The second aspect has to do with the minimum slope of the $V_{1/2}$ vs. $\log[Ca]_i$ relation. From Eq. 17 we see that for the simple system discussed above in which all electrical distances are equal the minimum possible slope is reached when δ is equal to 1. In this situation voltage is exerting its maximum possible effect on Ca^{2+} binding, and therefore, it takes a minimum change in voltage to compensate for a change in $[Ca]_i$. Substituting $\delta = 1$ into Eq. 17 the minimum slope is found to be -29.4 mV per 10-fold change in $[Ca]_i$. If we assume that each Ca^{2+} binding contributes positively towards channel activation, then this minimum slope applies to systems in which the δs are not all identical as well. This is because if at some binding sites δ values were <1, these binding steps would become less sensitive to voltage. It would take a larger change in voltage to compensate for the effect of changing $[Ca]_i$ at these sites, leading to a $V_{1/2}$ vs. $\log[Ca]_i$ relation which could only be more steep. Between 124 and 1,000 μM the slope of the mean $V_{1/2}$ vs. $\log[Ca]_i$ plot in Fig. 5 C is -28.9 mV per 10-fold change

Published May 1, 1997

in $[Ca]_i$. This result indicates that if the channel's voltage dependence lies solely in Ca^{2+} binding, all sites which contribute to channel activation must have a δ value close to 1.[2] If this is the case, however, a logarithmic relationship between $V_{1/2}$ and $[Ca]_i$ is predicted over the entire $[Ca]_i$ range, a prediction which is not born out in the data. So, a wide variety of models of activation by voltage-dependent Ca^{2+} binding are incompatible with our data and that of Wei et al. (1994). We can tentatively conclude, therefore, that there must be an intrinsic voltage sensor in the *mslo* protein that is distinct from Ca^{2+} binding.

Kinetic observations strengthen this conclusion. As was shown in Fig. 6 *E*, the macroscopic rate constant of *mslo* activation at +70 mV increases with increasing $[Ca]_i$ until a plateau is reached at high $[Ca]_i$ indicating a Ca-independent step is rate limiting. Plotted in Fig. 7 *A* are similar data for a series of voltages. Clearly, the effect of an increase in membrane voltage is to increase the maximum rate of activation, while otherwise having little effect on the shapes of these curves. This change in the maximum macroscopic activation rate constant (r_{max}) with voltage indicates that a Ca-independent step (or steps), most likely that which is limiting the *mslo* kinetic behavior at high $[Ca]_i$, is voltage dependent.

Considering SCHEME IV and Eq. 4 for example, if all of the channel's voltage dependence resided in either one or both Ca^{2+} binding steps, then at high $[Ca]_i$, regardless of the membrane voltage, r_{sat} would be simply equal to α. Depolarizing the membrane voltage would have no effect on r_{sat} but would reduce the amount of $[Ca]_i$ necessary to reach saturation. Conversely, if the channel's voltage dependence resided in the central Ca-independent conformational change, then, r_{sat} would increase with depolarization as $\alpha(V)$ increased, while less effect would be expected on the $[Ca]_i$ necessary to achieve saturation. For *mslo*, the apparent affinity, as defined by the $[Ca]_i$ necessary to half saturate the macroscopic activation rate constant, changes only to a small degree with changing voltage (Fig. 7 *C*), whereas r_{max} is voltage dependent (Fig. 7 *B*). These results are therefore most consistent with the voltage dependence of *mslo* gating residing in large part in Ca-independent steps.

To estimate the charge associated with Ca-independent steps, we might examine the voltage dependence of the macroscopic activation rate constant at saturating $[Ca]_i$ (Fig. 7 *B*). This is essentially what was done when a charge estimate was made from the voltage dependence of the time constant of activation at 1,000 μM (Fig. 2, *bottom*). Fitting the most depolarized region

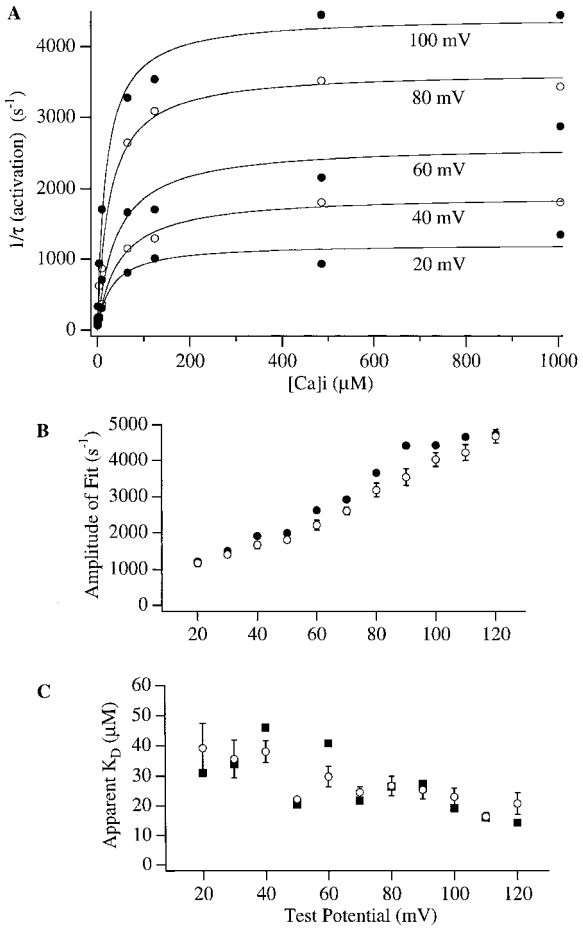

FIGURE 7. (*A*) The *mslo* macroscopic activation rate constant (1/time constant) is plotted as a function of $[Ca]_i$ for several different membrane voltages. Data are from a single membrane patch. Macroscopic rate constants were determined from exponential fits to the time course of activation. Voltages descend from top to bottom as indicated. Alternating open and closed markers have been used for ease of distinguishing data at differing voltages. Each data set has been fitted (*solid curve*) with the function $1/\tau = Amp/\{1+(K_D/[Ca]_i)\}$. To minimize the effects of outlying points an absolute, sum of squares criteria was used in fitting. The parameters from these fits, Amp (maximum macroscopic rate constant), and K_D (apparent Ca^{2+} dissociation constant) are plotted as a function of membrane voltage in *B* and *C* (●). Also included in *B* and *C* are mean values from 5 experiments (○). Error bars represent standard errors of the mean.

of this curve yielded a charge estimate of 0.58 ± 0.03 (SEM) *e* with a lower limit 0.39 ± 0.03 (SEM) *e* (Table II). We can conclude therefore that in the gating of the *mslo* channel there is at least this much charge associated with Ca-independent steps. If the reverse rate constants associated with these steps are also voltage dependent, this number would be an underestimate.

Ca^{2+} Binding Is Not Required for mslo Activation

If there are both Ca^{2+} and voltage sensing elements in the *mslo* protein, it is important to know whether the ac-

[2]Extreme cases can be found where this statement is not valid. In all such cases however it is necessary that the G-V relation be very strongly biphasic, drastically deviating from simple Boltzmann behavior. Since under no conditions does the *mslo* G-V relation show such biphasic character, such cases are not an issue here.

Published May 1, 1997

TABLE II

Rate Limiting Charge Estimates

	Forward		Backward	
$[Ca]_i$ (μM)	$\tau = Ae^{-q_f FV/RT} + b$ q_f	$\tau = Ae^{-q_f FV/RT}$ q_f	$\tau = Ae^{q_b FV/RT} + b$ q_b	$\tau = Ae^{q_b FV/RT}$ q_b
0.84	0.76 ± 0.113* (4)‡	0.43 ± 0.026* (4)‡	0.66 ± 0.029* (7)‡	0.49 ± 0.101 (7)
1.7	0.73 ± 0.021 (10)	0.42 ± 0.012 (10)	0.62 ± 0.030 (6)	0.44 ± 0.060 (6)
4.5	0.78 ± 0.027 (9)	0.48 ± 0.020 (9)	0.60 ± 0.016 (7)	0.45 ± 0.062 (7)
10.2	0.67 ± 0.025 (7)	0.49 ± 0.016 (7)	0.66 ± 0.029 (10)	0.48 ± 0.065 (10)
65	0.66 ± 0.049 (8)	0.50 ± 0.038 (8)	0.67 ± 0.039 (6)	0.44 ± 0.040 (6)
124	0.65 ± 0.032 (7)	0.46 ± 0.028 (7)	0.67 ± 0.030 (9)	0.46 ± 0.054 (9)
490	0.59 ± 0.029 (7)	0.47 ± 0.026 (7)	0.65 ± 0.021 (9)	0.41 ± 0.050 (9)
1000	0.58 ± 0.031 (5)	0.39 ± 0.028 (5)	0.64 ± 0.015 (10)	0.41 ± 0.042 (10)

*Values are given as mean ± standard error. ‡In parentheses is the number of experiments used to determine each value.

tivation of either or both types of elements is necessary for the channel to open. To address the question of whether $[Ca]_i$ binding is necessary, we have looked for *mslo* currents at very low $[Ca]_i$. When Ca^{2+} is omitted from our standard internal solution, and no Ca^{2+} chelator is added, we have measured the free Ca^{2+} concentration to be between 10 and 20 μM. Adding 5 mM EGTA to this solution should then bring $[Ca]_i$ to ~0.5 nM (pH = 7.20, apparent Ca^{2+} K_D 160 nM calculated from the stability constants of Fabiato and Fabiato [1979]). Fig. 8 *A* shows *mslo* currents recorded using such a low $[Ca]_i$ solution. The membrane voltage was held at −50 mV and then stepped to increasingly more positive voltages (+50 to +200 mV). Up until +90 mV, no significant current was observed. At more positive potentials, however, a large time-dependent outward current developed. The size of this current increased with depolarization, and at +200 mV was typically equal to 69 ± 7% (SEM) ($n = 5$) of the *mslo* current recorded from the same patch with 124 μM $[Ca]_i$ (Fig. 8 *B*). Several lines of evidence indicate that this current is passing through *mslo* channels: It is not present in uninjected oocytes (Fig. 9 *A*). From patch to patch its size correlates well with the amplitude of Ca-dependent currents recorded with 124 μM $[Ca]_i$ (Fig. 9 *B*). It is almost completely and reversibly blocked by 3 mM external TEA as is expected for the *mslo* channel (Butler et al., 1993) (Fig. 9 *C*), and, its single channel conductance is large, and identical to that of *mslo* (Fig. 9 *D*). In addition to these observations Palotta (1985*b*) and Meera et al. (1996) have reported low probability BK channel opening at very low [Ca].

It appears, then, that the *mslo* channel can open without binding Ca^{2+}. However, it could be that there are voltage-dependent Ca^{2+} binding sites on the *mslo* channel, and at the extreme voltages necessary to activate the channel with ~0.5 nM $[Ca]_i$, the affinity of these sites for Ca^{2+} increases to such an extent that a significant fraction of channels have Ca^{2+} bound. Consider-

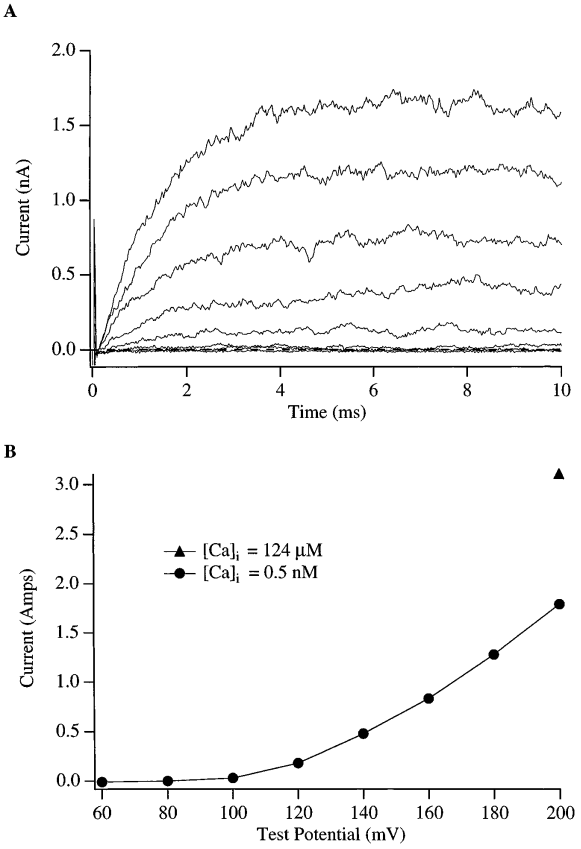

FIGURE 8. *mslo* currents at very low $[Ca]_i$. (*A*) Currents were elicited with depolarizing steps to test potentials ranging from +60 to +200 mV in 20-mV increments. V_{hold} = −50 mV. Included in the internal solution was 5 mM EGTA. No HEDTA or Ca^{2+} was added. The calculated free $[Ca]_i$ in this solution was ~0.5 nM assuming contaminant Ca^{2+} of 10 to 20 μM (see MATERIALS AND METHODS). The traces displayed are the average from 5 series recorded consecutively. (*B*) Peak current values from the data in *A* are plotted as a function of membrane voltage (●). Also included is the peak current measured from the same patch with a step to +200 mV while the patch was superfused with 124 μM $[Ca]_i$ (▲).

Published May 1, 1997

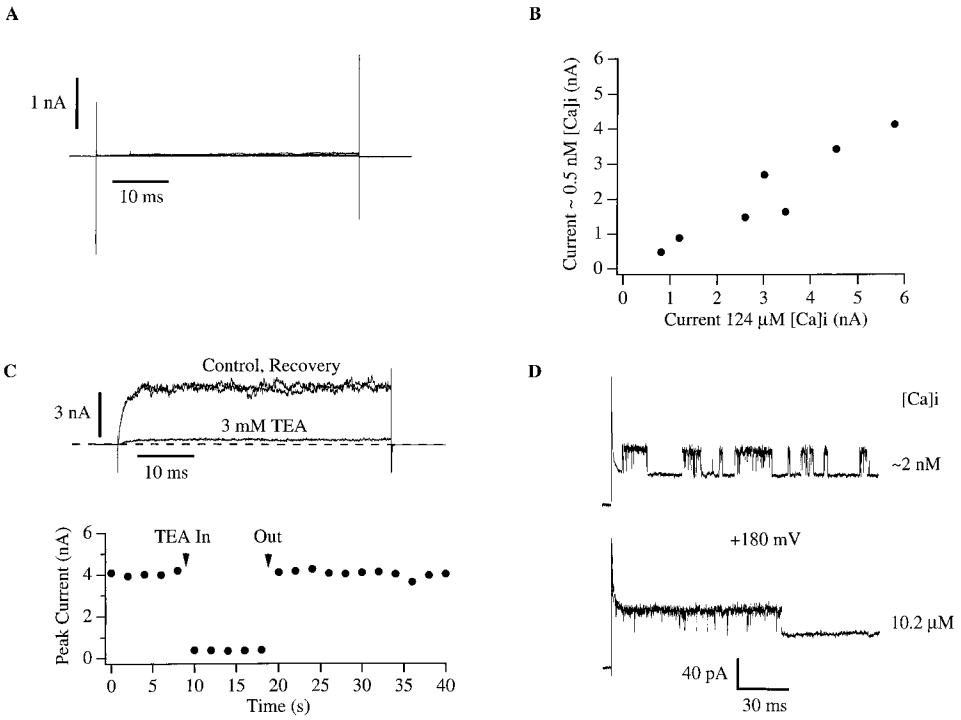

FIGURE 9. Currents recorded at high voltage and very low $[Ca]_i$ are passing through *mslo* channels. (*A*) Control currents recorded from an oocyte not injected with RNA. Currents shown were elicited with 50-ms voltage steps to potentials ranging from +60 to +200 mV in 20-mV increments. $V_{hold} = -50$ mV. (*B*) Correlation between the amplitudes of *mslo* currents recorded from the same patches with ~0.5 nM (*ordinate*) or 124 μM (*abscissa*) $[Ca]_i$. Each symbol represents an individual experiment. Amplitudes were measured at the end of 50-ms depolarizations to +200 mV. $V_{hold} = -50$ mV (0.5 nM $[Ca]_i$); $V_{hold} = -120$ mV (124 μM $[Ca]_i$). (*C*) Current traces recorded from an outside out membrane patch with voltage steps to from −50 to +200 mV before (*control*), during (*3 mM TEA*), and after (*recovery*) exposure of the external surface of the patch to 3 mM TEA. In the lower panel the time course of TEA block is displayed. Data points were recorded at 2-s intervals. (*D*) Single channel current traces recorded from inside out membrane patches pulled from oocytes injected with a low concentration of *mslo* RNA, at ~2 and 10.2 μM $[Ca]_i$. Voltage steps were to +180 mV.

ing for example a Ca^{2+} binding site with an electrical distance of 0.8, at +180 mV the dissociation constant for this site would decrease by a factor of 1.25×10^5 as compared to its value at 0 mV, moving perhaps from 10 μM to 0.125 nM. Such a site would be 80% occupied at 0.5 nM $[Ca]_i$. The question then remains open as to whether Ca^{2+} must bind to the channel before it will open.

More can be learned about this question when the rate of activation at very low $[Ca]_i$ is considered. Fig. 10 shows two current traces recorded from the same membrane patch, one at 10.2 μM $[Ca]_i$ after a voltage step to +170 mV, and the other at ~0.5 nM $[Ca]_i$ (5 mM EGTA) after a voltage step to +250 mV. At 10.2 μM $[Ca]_i$ the voltage step to +170 mV fully activates the channels as can be seen by examining the G-V relation determined at 10.2 μM in Fig. 5. Judging by the similar amplitudes of the traces recorded at 10.2 μM and ~0.5 nM $[Ca]_i$ in Fig. 10, the voltage step to +250 mV with ~0.5 nM $[Ca]_i$ must have brought the *mslo* channels near to their maximum open probability as well (differences in driving force here are not an issue as the *mslo* single channel current saturates at potentials above ~+120 mV, see Cox et al., 1997, in this issue). The trace recorded with ~0.5 nM $[Ca]_i$ has been fitted with an exponential function (*dashed curve*) whose time constant is 1.15 ms. In six similar experiments the mean time constant of activation under these conditions was 1.4 ms ± 0.36 (SD). In these experiments the Ba^{2+} chelator (+)-18-crown-6-tetracarboxylic acid was added to the internal solution to reduce the possibility of Ba^{2+} block altering current kinetics (Diaz et al., 1996; Neyton, 1996) (although such effects are likely to be small, Cox et al., 1997). At high open probability, such as is the case here (see Figs. 5 and 8 in Cox et al., 1997), the above time constant (1.4 ms) represents the mean time it takes for an *mslo* channel to move from closed to open after the voltage step. This can be made more explicit by considering that at high open probability rates entering open states are necessarily much larger than rates leaving open states so that the rate of change of the current ($d[I/I_{max}]dt$) becomes very close to the rate of arrival of channels into open states. The mean transit time (m_t) from closed to open is given by

$$m_t \cong \int_0^\infty \frac{d[I/I_{max}]}{dt} t\, dt. \qquad (18)$$

In the present case, where the timecourse of current activation is described by an exponential function with time constant τ, we have

$$m_t \cong \int_0^\infty \frac{d[1-e^{-t/\tau}]}{dt} t\, dt, \qquad (19)$$

Published May 1, 1997

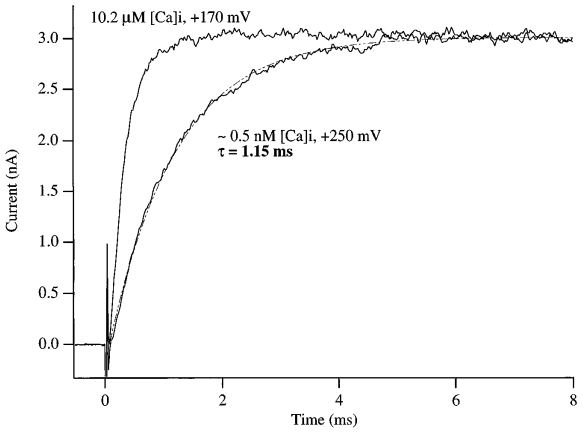

FIGURE 10. Rapid activation of *mslo* currents at very low $[Ca]_i$. The two current traces displayed were recorded from the same membrane patch with 10.2 μM and ~0.5 nM $[Ca]_i$ (5 mM EGTA no added Ca^{2+}) as indicated. The traces shown represent the average of 5 (10.2 μM $[Ca]_i$) and 8 (~0.5 nM $[Ca]_i$) traces recorded in consecutive current families. Voltage steps were from −100 to +170 mV at 10.2 μM $[Ca]_i$, and from 0 to +250 mV at ~0.5 nM $[Ca]_i$. The ~0.5 nM $[Ca]_i$ trace was fitted with a single exponential function with a time constant of 1.15 ms. The fit is superimposed on the data (*dashed line*).

$$m_t \cong \frac{1}{\tau}\int_0^\infty e^{-t/\tau} t \, dt, \tag{20}$$

whose solution is

$$m_t \cong \tau, \tag{21}$$

demonstrating that the mean time for a channel to move from closed to open after the voltage step under these conditions will closely correspond to the time constant of current activation. Inverting the *mslo* activation time constant at ~0.5 nM $[Ca]_i$ and +250 mV (1.4 ms) yields a first order rate constant of 714 s^{-1}. All the elementary transitions that the channel undergoes on its way to opening, therefore, must have rate constants at least this rapid, and if Ca^{2+} must bind to the channel after the voltage step and before opening, then Ca^{2+} must bind at least this fast as well. The rate of Ca^{2+} binding, however, depends on its concentration. At 0.5 nM in order for Ca^{2+} to bind to the channel with a first order rate constant of 714 s^{-1}, the second order rate constant for Ca^{2+} binding must be at least 1.4×10^{12} $M^{-1}s^{-1}$. Is this a reasonable on rate? We might use the expression of Smoluchowski (1916) below to calculate the diffusion limited on rate constant for the Ca^{2+} binding reaction.

$$k_{on} = \frac{2\pi N_A D_{Ca} r_o}{1{,}000}. \tag{22}$$

Here N_A represents Avogadro's number, D_{Ca} the diffusion coefficient of Ca^{2+}, and r_o the reaction radius (the distance between reacting particles at the point of collision). Considering that D_{Ca} equals 0.79×10^{-5} cm^2s^{-1}, at 25°C (Hille, 1992), and r_o is on the order of a few angstroms (Pauling radius of Ca^{2+} = 0.99 Å, Pauling radius of oxygen = 1.40 Å), the diffusion limited k_{on} is on the order of 10^9 $M^{-1}s^{-1}$. This value is three orders of magnitude smaller than the value experimentally determined above to be necessary to allow time for Ca^{2+} to bind to its site after the voltage step and activate the channel. This result therefore suggests that the *mslo* channel can be activated by a change in membrane voltage without binding Ca^{2+}. This rate limiting value, however, is calculated based on simple diffusion alone. No electrical driving force is taken into the consideration. If the Ca^{2+} binding site is in the electric field, the diffusion-limited rate at which Ca^{2+} approaches its binding site may be increased due to the electrical driving force the field imparts on the ion with a factor of about $zF\Psi/RT$, where $z = 2$ is the valence of Ca^{2+}, Ψ is the potential near the binding site, and F, R, and T have their usual meanings (Getzoff et al., 1992; Pilling and Seakins, 1995). The negative surface potential near the Ca^{2+} binding site on the intracellular face of the membrane (Frankenhaeuser and Hodgkin, 1957; Chandler et al., 1965) may contribute to this driving force. The contribution of the surface potential should be <−90 mV (Hille et al., 1975). This would enhance the Ca^{2+} binding rate to a value of 7×10^9 $M^{-1}s^{-1}$. This limit is still ~200 times smaller than the value necessary to account for the rapid activation kinetics observed (1.4×10^{12} $M^{-1}s^{-1}$).

Other evidence that indicates that at very low $[Ca]_i$ the *mslo* channel can be activated by voltage without first binding Ca^{2+} comes from experiments in which $[Ca]_i$ was varied in the low nanomolar range. Several internal solutions were prepared with the following calculated free $[Ca]_i$: 0.5 nM (no added Ca^{2+}, 5 mM EGTA), 2 nM (no added Ca^{2+}, 1 mM EGTA,), 10 nM (0.28 mM added $CaCl_2$, 5 mM EGTA), and 50 nM (1.18 mM added $CaCl_2$, 5 mM EGTA). *mslo* currents were then recorded from a single membrane patch using each of these solutions. The rationale behind this experiment was that if at very low $[Ca]_i$ (~0.5 nM) and high voltage, it is Ca^{2+} binding that is activating the *mslo* channel, then we would expect to see changes in the amplitude and time course of *mslo* currents as $[Ca]_i$ is varied in the low nanomolar range. I-V curves from one such experiment are shown in Fig. 11 *A*. The clear result is that there was no significant increase in the amplitudes of currents recorded with internal solutions containing 2 or 10 nM $[Ca]_i$ over those recorded with ~0.5 nM $[Ca]_i$. Nor was there a clear increase in activation rate. (Fig. 11 *B*). The same result was obtained in five additional experiments, all supporting the conclu-

Published May 1, 1997

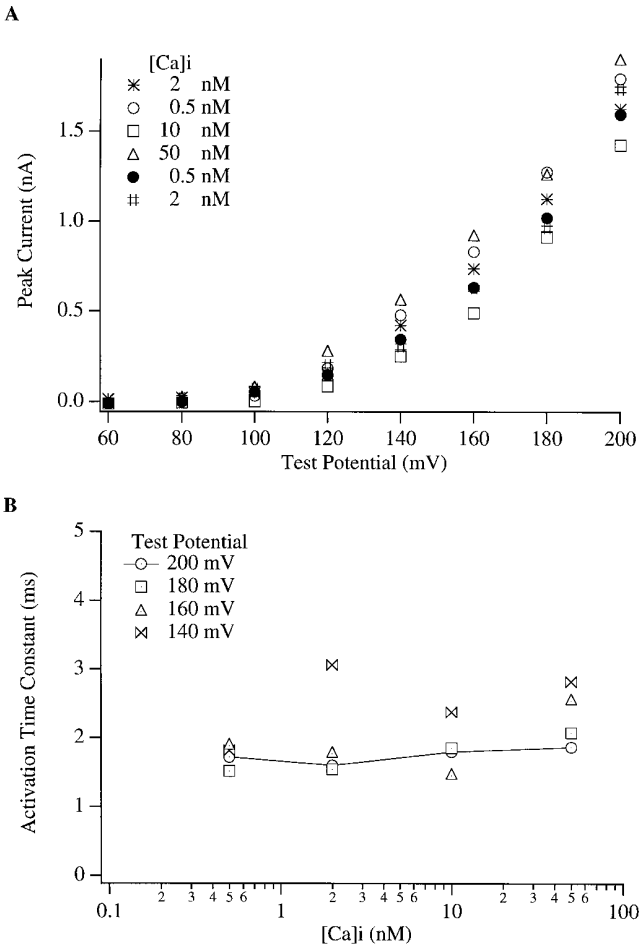

FIGURE 11. *mslo* currents are insensitive to changes in $[Ca]_i$ in the low nanomolar range. (*A*) *mslo* currents recorded from a single membrane patch at the indicated $[Ca]_i$. Internal solutions were prepared from the standard solution as follows: 0.5 nM (no added Ca^{2+}, 5 mM EGTA), 2 nM (no added Ca^{2+}, 1 mM EGTA), 10 nM (0.28 mM added $CaCl_2$, 5 mM EGTA), 50 nM (1.18 mM added $CaCl_2$, 5 mM EGTA). The order of solution presentation was as follows 2 nM (*), 0.5 nM (○), 10 nM (□), 50 nM (△), 0.5 nM again (●), 2 nM again (#). (*B*) Time constants of activation for currents in *A* are plotted as a function $[Ca]_i$. Each symbol represents data from a different test potential as indicated. The data points at +200 mV have been connected (*solid line*). Time constants were determined by fitting the time course of activation with a single exponential function.

sion that at very low $[Ca]_i$ the channel is opening without binding Ca^{2+}. These results also indicate that if surface charges are concentrating Ca^{2+} near its binding sites, then the channels are not sensitive to changes in the surface charge enhanced Ca^{2+} concentration as well. This is because the relationship between $[Ca]_{bulk}$ and that which is concentrated by surface charge is expected to be linear. At 50 nM $[Ca]_i$ a small increase in current amplitude relative to that at 0.5, 2, or 10 nM was observed suggesting that at this $[Ca]_i$ the *mslo* channels may be just starting to bind Ca^{2+} appreciably.

To guard against errors in solution making, we measured the Ca^{2+} concentrations in the solutions employed in the experiment of Fig. 11 using the Ca^{2+} indicator fura II (100 μM) with the following results: calculated 0.5 nM, measured 0 nM; calculated 2 nM, measured 0 nM; calculated 10 nM, measured 1 nM; calculated 50 nM, measured 63 nM. The precision of these measurements, ± 20 nM, was limited by the sensitivity of the indicator. Nevertheless, they do confirm that the free Ca^{2+} concentrations in these solutions are in the high picomolar to low nanomolar range.

mslo Can Be Nearly Maximally Activated without Binding Ca^{2+}

The experiments described above strongly support the conclusion that the *mslo* channel has intrinsic voltage sensing elements and that the action of these elements is sufficient to activate the channel substantially. In fact the similar amplitudes of the traces in Fig.10 argue that with strong depolarizations the *mslo* channel can be maximally activated without binding $[Ca]_i$. More evidence to support this conclusion is shown in Fig. 12 *B*. Here G-V relations determined from patches exposed to both 10.2 μM (*squares*) and ~0.5 nM $[Ca]_i$ (*circles*) are displayed. To maximally activate *mslo* channels at ~0.5 nM $[Ca]_i$, it was necessary to depolarize to potentials greater than +200 mV. In 6 of 17 experiments, voltages as high as +250 mV were attained (*closed circles*). In 3 experiments it was possible to depolarize to +280 mV (*open circles*). At this potential the maximum current observed with ~0.5 nM $[Ca]_i$ was on average 101 ± 6% (SD) of that measured with 10.2 μM $[Ca]_i$ at +150 mV (Fig. 12 *A*). Because the *mslo* channel's single channel current saturates ~+120 mV (see Cox et al., 1997, in this issue), current amplitude and open probability at these high voltages become directly comparable. These results therefore indicate that, in contrast to the low probability openings reported previously in extremely low $[Ca]_i$ and lower voltages (Pallotta, 1985*a*; Meera et al., 1996), by +280 mV the *mslo* channels were very close to being fully activated.

The mslo G-V Relation Is Less Steep at Very Low $[Ca]_i$ than It Is at 10.2 μM $[Ca]_i$

The data in Fig. 12 *B* also allow a comparison to be made between the shape of the *mslo* G-V relation under conditions in which the channel is activating without binding Ca^{2+} (~0.5 nM $[Ca]_i$) to that observed with $[Ca]_i$ sufficient to regulate channel gating (10.2 μM $[Ca]_i$). In this experiment (+)-18-crown-6-tetracarboxylic acid was included in the internal solution to ensure that the shape of the G-V relation was not distorted by Ba^{2+} block. Also, to control for time-dependent changes unrelated to changes in $[Ca]_i$, in each experiment current families were recorded at 10.2 μM $[Ca]_i$ before

Published May 1, 1997

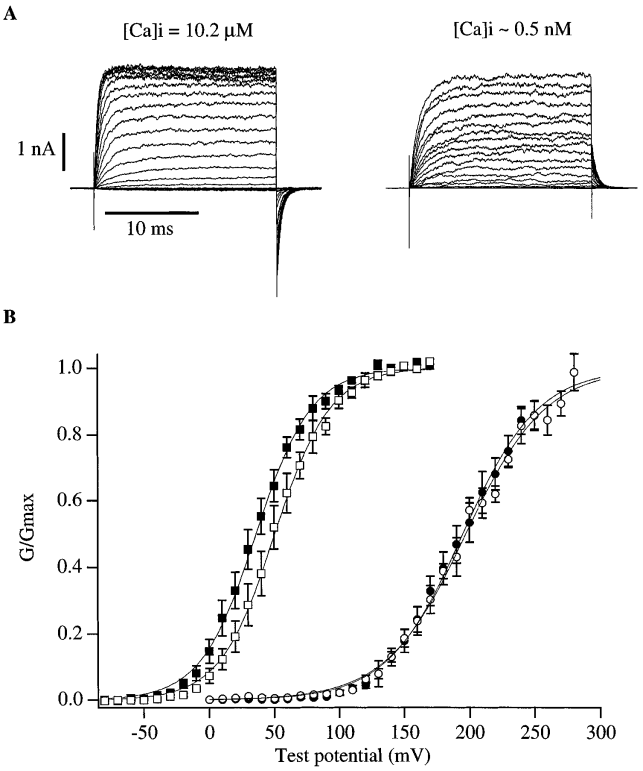

FIGURE 12. (A) *mslo* current families recorded from the same membrane patch at 10.2 μM and ~0.5 nM $[Ca]_i$. Each family displayed is the average of 5 (10.2 μM) and 8 (~0.5 nM) families recorded in succession. (*B*) Mean *mslo* G-V curves recorded from 6 membrane patches with 10.2 μM $[Ca]_i$ before (■) and after (□) superfusion with ~0.5 nM $[Ca]_i$ (●). In three patches current families were determined with ~0.5 nM $[Ca]_i$ with voltages up to +280 mV (○). Error bars represent standard errors of the mean. G-V curves were fit with the Boltzmann function $G = G_{max}(1/\{1+e^{-(V-V_{1/2})zF/RT}\})$ and then normalized to the maximum of the fit. Fit parameters were as follows: (■) $V_{1/2}$ = 36 mV, z = 1.18; (□) $V_{1/2}$ = 50 mV, z = 1.19; (●) $V_{1/2}$ = 195 mV, z = 0.87; (○) $V_{1/2}$ = 197 mV, z = 0.83.

(*filled squares*) and after (*open squares*) families with ~0.5 nM $[Ca]_i$ (*filled circles*). Each set of data in Fig. 12 *B* is fitted with a Boltzmann function of the form $G/G_{max} = 1/(1+e^{zF(V_{1/2}-V)/RT})$. The equivalent gating charge estimates determined from these fits were 1.18 *e* (before) and 1.19 *e* (after) for the G-V relations determined with 10.2 $[Ca]_i$, and 0.87 *e* (voltages to +250 mV) and 0.83 *e* (voltages to +280 mV) for those measured with ~0.5 nM $[Ca]_i$. These numbers suggest that the *mslo* channel is less sensitive to changes in membrane voltage when gating without Ca^{2+} binding than it is in the presence of 10.2 μM $[Ca]_i$. There is an apparent 26 to 31% decrease in equivalent gating charge at low $[Ca]_i$.

We have considered three possible explanations for this observation. The first is that while most of the gating charge of the channel derives from intrinsic voltage sensing elements, Ca^{2+}, as it binds to the channel, may bind a short distance into the electric field ($\delta < 0.2$) and therefore contribute approximately a quarter to a third of the total gating charge. Second, as pointed out by Zagotta et al. (1994*a*), the steepness of a channel's G-V relation depends not only on the amount of charge moved through the membrane's electric field during opening but also on the cooperativity of gating conformational changes. The decrease in maximum G-V slope observed at low $[Ca]_i$ therefore might be attributed to Ca-dependent changes in the cooperative interactions between subunits, rather than to a change in gating charge. And third, the more shallow maximum G-V slope at ~0.5 nM $[Ca]_i$ as compared to 10.2 μM $[Ca]_i$ may be not so much a consequence of the change in $[Ca]_i$, as it is a consequence of the fact that when gating in a Ca-independent way, the *mslo* G-V relation spans extreme positive potentials. It may be that the equivalent gating charge of the channel changes as a function of the voltage range examined. A physical interpretation of such a phenomenon might be that there is a change in polarizability of the channel between open and closed states such as might come about if dipoles can be induced by the electric field in one state and not the other (Stevens, 1978; Sigworth, 1994). Such a change in polarizability would make the work done when the channel moves from closed to open a nonlinear function of voltage (Stevens, 1978) and could result in a more shallow G-V relation at extreme potentials. Unfortunately, at present we are unable to distinguish between these possibilities. In the future, however, experiments involving gating current measurements and the study of mutant channels whose G-V relations at low $[Ca]_i$ are shifted to more hyperpolarized potentials may help make such a distinction possible. At present, however, the most we can say is that the *mslo* channel retains ~70% of its apparent voltage sensitivity at very low $[Ca]_i$ as estimated by simple Boltzmann fitting.

Voltage Appears to Limit the Extent to which Ca^{2+} Can Activate the mslo Channel

The results of experiments with very low $[Ca]_i$ demonstrate that a lack of $[Ca]_i$ does not limit the extent to which *mslo* channels can be activated by voltage provided sufficiently large depolarizations are used. It is important to ask whether the converse is true. Can a high enough $[Ca]_i$ maximally active *mslo* channels regardless of the membrane voltage? We can see from the G-V curves of Fig. 5 that the answer to this question is likely to be no. Even with 1,000 μM $[Ca]_i$, applying a membrane voltage of −180 mV essentially completely prevented the *mslo* channels from opening.

The ability of membrane voltage to limit the extent to which *mslo* channels can be activated by $[Ca]_i$ can be better seen when steady-state open probability (P_o) is plotted as a series of Ca^{2+} dose response curves (Fig. 13

Published May 1, 1997

A). Here, the curves from top to bottom correspond to data taken at successively more negative voltages in increments of 20 mV. Each curve has been fitted with the Hill equation (Eq. 1). At +90 mV (*top curve*) the channels are essentially fully activated by 10.2 μM $[Ca]_i$ and the fitted curve approaches 1 on the ordinate. Near full activation is also reached at +50 mV (*third from top*), although here it takes more Ca^{2+} to bring the channels to full open. By −10 mV (*third from bottom*), however, the fitted curve reaches a maximum below 1 on the ordinate, and when the maximum of each fit is plotted as a function of voltage (Fig. 13 *B*), the fraction of channels which can be activated decreases with decreasing voltage. These data therefore suggest that negative potentials can limit the ability of $[Ca]_i$ to activate *mslo*. Some studies, however, indicate that the BK channel G-V relation moves further leftward along the voltage axis with increases in $[Ca]_i$ above the maximum $[Ca]_i$ we have used (1,000 μM) (Moczydlowski and Latorre, 1983; Meera et al., 1996). That we have reached saturation of the *mslo* channel's Ca^{2+} binding sites by 1,000 μM $[Ca]_i$ is therefore not clear. Wei et al.(1994) have suggested that leftward G-V curve shifts above ~100 μM $[Ca]_i$ are due to a nonspecific divalent cation binding site rather than the channel's primary Ca^{2+} sensors, and that saturation of the primary site is reached by ~100 μM $[Ca]_i$. Because of these complications, we can only tentatively conclude that membrane voltage limits the ability of $[Ca]_i$ to activate the *mslo* channel at negative potentials.

How Many Ca^{2+} Molecules Bind to the Channel?

To gain further insight into the Ca^{2+}-dependent activation of *mslo* it would be useful to know how many Ca^{2+} binding sites there are on the channel. We can determine a lower limit for this number by considering the Hill coefficients determined from fitting the Ca^{2+} dose response curves in Fig. 13 *A*. In general for a system with *N* binding sites, this coefficient will be less than or equal to *N* (Adair, 1925). In Fig. 13 *C* are plotted Hill coefficients as a function of voltage for both the data in Fig. 13 *A* (*filled circles*) and the mean of five similar experiments (*open circles*). The trend in these data is toward larger Hill coefficients at more depolarized voltages. Over the majority of the voltage range the Hill coefficient varied between 1 and 3 clearly indicating that at least three Ca^{2+} binding sites are associated with channel activation.

In Fig. 13 *D* the apparent K_D of the channel for Ca^{2+} as determined from fits to the Hill equation is plotted

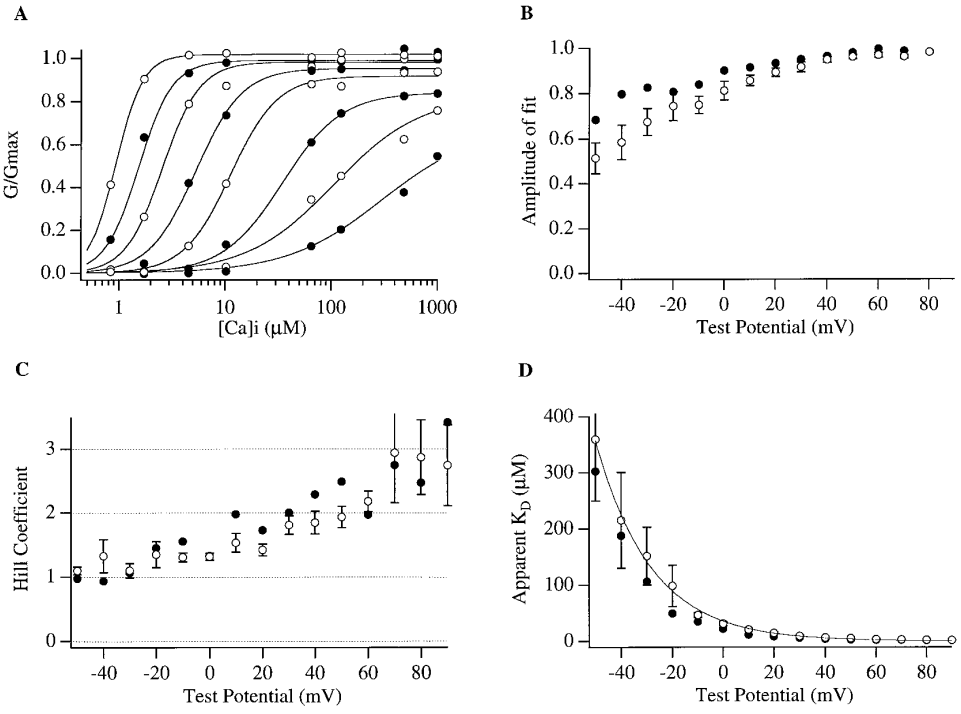

FIGURE 13. Ca-dependence of *mslo* currents. (*A*) Conductance vs. voltage (G-V) relations at the following $[Ca]_i$: 0.84, 1.7, 4.5, 10.2, 65, 124, 490, 1,000 μM where constructed from tail current amplitudes measured 0.2-ms after repolarization from the appropriate test potential to −80 mV. Each G-V curve was then fitted with a Boltzmann function and normalized to the maximum of the fit. These data were transformed to dose-response form for each voltage and displayed in *A*. Smooth curves represent fits to the Hill equation $G/G_{max} = Amp/\{1+(K_D/[Ca])^n\}$, were n = Hill coefficient, and K_D = apparent Ca^{2+} dissociation constant. Voltages descend from left to right starting at +90 mV and ending at −50 mV in 20-mV increments. Alternating open and closed markers have been used for ease of distinguishing data at differing voltages. The data are from the same membrane patch. In (*B*) the amplitudes of each fit in *A* are plotted as a function of voltage. In (*C*) Hill coefficients, and in (*D*) apparent dissociation constants determined from the curves in *A* are also plotted as a function of voltage. In *B*, *C*, and *D* closed circles represent parameters determined from the fits in A. Open circles represent the mean values from 5 experiments. The mean data in *D* have been fitted (*solid line*) with the function $K_D(V) = K_D(0)e^{-zFV/RT}$ with $K_D(0)$ = 35.2 μM and z = 1.18. Error bars indicate standard errors of the mean.

Published May 1, 1997

as a function of membrane voltage. As expected from the shifting behavior of the *mslo* G-V relation in response to changes in $[Ca]_i$, the apparent K_D declines sharply with increasing voltage. The mean data (*open circles*) have been fitted with an exponential function which changes *e*-fold per 21.6 mV.

DISCUSSION

Intrinsic Voltage Sensing

In this study we have examined macroscopic *mslo* currents over a wide range of membrane voltages and Ca^{2+} concentrations to address some fundamental questions about the channel's gating mechanism. One important question related to BK channel gating is whether the channel's voltage dependence derives from intrinsic gating charges which are part of the protein sequence or instead from voltage-dependent Ca^{2+} binding? A leading model from single channel studies of skeletal muscle BK channels has suggested that the channel's voltage dependence resides in Ca^{2+} binding (Moczydlowski and Latorre, 1983). With the cloning of *slo* channels (Atkinson et al., 1991; Adelman et al., 1992; Butler et al., 1993), however, it became apparent that BK channels contain an S4 region which in purely voltage-gated channels is thought to span the membrane and form at least a part of an intrinsic voltage sensor (Stuhmer et al., 1989; Liman et al., 1991; Papazian et al., 1991; Perozo et al., 1994; Sigworth, 1994; Smith-Maxwell et al., 1994; Yang and Horn, 1995; Aggarwal and MacKinnon, 1996; Larsson et al., 1996; Mannuzzu et al., 1996; Seoh et al., 1996; Yang et al., 1996). These results suggested that *slo* channels may contain intrinsic voltage-sensing elements like those of the *shaker* channel. The *shaker* channel, however, contains seven basic residues in this region, whereas *slo* channels have only four. The reduced number of basic residues, therefore, might reasonably have rendered the *slo* channels' S4 regions no longer able to sense changes in membrane potential. Furthermore, the presence of an S4 region does not ensure that a channel will exhibit voltage-dependent gating. For example, the cyclic-nucleotide–gated channel of rod outer segment also has structural similarity to *shaker* channels including S4 and pore regions; this channel contains 5 positive charges in its S4 region (Kaupp et al., 1989), yet shows very little voltage dependence (Karpen et al., 1988).

In this study we provide three lines of evidence which indicate that the *mslo* channel does indeed have intrinsic voltage sensing elements which are distinct from Ca^{2+} binding. The first is that the position of the *mslo* G-V relation does not vary logarithmically with $[Ca]_i$. This observation is in support of the work of Wei et al. (1994), who also observed smaller shifts in the position of the *mslo* G-V relation per 10-fold change in $[Ca]_i$ at high $[Ca]_i$ than at low $[Ca]_i$. As they pointed out, it is difficult to find markovian models whose $V_{1/2}$ vs. $\log[Ca]_i$ relation is not linear if voltage dependence is assigned only to Ca^{2+} binding steps and these Ca^{2+} binding steps have approximately equal voltage dependence. Extending their analysis, we have shown that for all systems whose voltage dependence resides solely in Ca^{2+} binding, a logarithmic relationship between $V_{1/2}$ and $[Ca]_i$ is expected so long as the electrical distances of all binding sites are the same (this was shown for a sequential binding model by Wong et al. [1982]). Given that we and others have observed Hill coefficients as high as 3, and evidence suggests that *slo* α subunits expressed alone form homotetrameric channels (Shen et al., 1994), it is reasonable to suppose that *slo* channels contain four identical Ca^{2+} binding sites, one per subunit. In such systems all binding sites naturally have equivalent electrical distances unless cooperative interactions between subunits serially alter the position of Ca^{2+} binding sites as each new Ca^{2+} molecule binds to the protein. Even without relying on simple symmetry, however, between 124 and 1,000 μM $[Ca]_i$ the slope of the $V_{1/2}$ vs. $\log[Ca]_i$ relation is so shallow as to require that, if the channel's voltage dependence were to reside solely in Ca^{2+} binding steps, the electrical distance of each binding site would have to be close to 1. If this were the case, however, the $V_{1/2}$ vs. $\log[Ca]_i$ relation would necessarily be linear. This contradiction indicates that there must be some gating charge associated with conformational changes which do not involve Ca^{2+} binding.

Further supporting this conclusion, we have found that the macroscopic rate constant of *mslo* activation approaches saturation at high $[Ca]_i$. This saturating behavior indicates that gating transitions which do not involve Ca^{2+} binding are limiting the kinetic behavior of the *mslo* channel at high $[Ca]_i$. The fact that the maximum value of this limiting rate is voltage dependent, as was shown in Fig. 7, indicates that transitions that are separate from Ca^{2+} binding are necessarily voltage dependent, and thus, there must be gating charges intrinsic to the channel.

The third line of evidence in support of intrinsic voltage sensing is the observation that *mslo* channels can be substantially activated with $[Ca]_i$ as low as ~0.5 nM. This observation agrees with several reports of low probability BK channel activity at very low $[Ca]_i$ (Barrett et al., 1982; Methfessel and Boheim, 1982; Wong et al., 1982; Findlay et al., 1985; Pallotta, 1985*b*; Meera et al., 1996). In fact, we have found that with depolarizations to +280 mV the *mslo* channels can be nearly maximally activated at ~0.5 nM $[Ca]_i$, indicating that a lack of Ca^{2+} binding does not limit the ability of the channel to be activated by voltage. It is clear that this activation is truly Ca^{2+} independent, rather than due to very

Published May 1, 1997

high affinity Ca^{2+} binding, because the time constant of current activation at ~0.5 nM $[Ca]_i$ is three orders of magnitude faster than the mean diffusion-limited time it would take Ca^{2+} to find its binding site after a depolarizing voltage step.

From the above analysis it is clear that, at very low [Ca], Ca^{2+} is not binding to and activating the *mslo* channels after the voltage step. We considered the possibility, however, that in the essential absence of Ca^{2+}, some other ion in our internal solution was binding to Ca^{2+} binding sites and activating the channels. Oberhauser et al.(1988) have reported the following rank order of activating ions for skeletal muscle BK channels: Ca^{2+} ($K_D = 8.98 \times 10^{-4}$ mM) >> Cd^{2+}(K_D = 0.27 mM) > Sr^{2+}(K_D = 0.73 mM) > Mn^{2+}(K_D = 0.96 mM) > Fe^{2+}(K_D = 2.7 mM) > Co^{2+}(K_D = 3.81 mM). K_D here indicates half-saturating ion concentration at +80 mV. Excepting Ca^{2+}, none of these ions were added to our internal solutions. Some of them, however, may have entered into these solutions as a contaminant. To check this point the total concentrations of the most potent of these ions were measured by atomic absorption spectroscopy (AA). Cd^{2+}, Sr^{2+}, and Mn^{2+} were not detected indicating that if present their concentrations were lower than the resolution of the assay (~0.3 μM). Iron was present at 4.56 μM. Given these results one might still suppose that Cd^{2+}, Sr^{2+}, or Mn^{2+} present at just below the AA detection limit, or perhaps Fe^{2+}, is able to rapidly activate *mslo* channels at high voltages. EGTA however has high affinity for all of these ions, and calculations of the maximum possible free concentrations of these ions in our internal solution containing 5 mM EGTA indicates that only Sr^{2+} could be present at a free concentration higher than Ca^{2+}, and then only at ~1.3 nM. This concentration is still too small to account for the rapid activation of *mslo* currents in the presence of 5 mM internal EGTA. Based on these results we do not believe that in our low $[Ca]_i$ experiments the *mslo* channels are being activated by a contaminant ion.

Our conclusion that the *mslo* channel has intrinsic voltage sensors differs from the mechanism proposed by Moczydlowski and Latorre (1983) for the voltage-dependent gating of a skeletal muscle BK channel. They concluded that this channel's voltage dependence comes from the voltage dependence of Ca^{2+} binding. There are several differences between the two studies including: native skeletal muscle channels vs. cloned α subunits expressed alone in oocytes, and single channel vs. macroscopic currents. However, the manner by which Moczydlowski and Latorre plotted their data may have made the intrinsic voltage dependence of the channel they studied less apparent. Their conclusion was based primarily on the observations that the channel's mean open time (τ_{open}) and mean closed time (τ_{closed}) were not clearly voltage dependent when extrapolated to $[Ca]_i = 0$ and $1/[Ca]_i = 0$, respectively. However, at these extremes the mean open and closed times are at their minimum. Voltage-dependent changes in these values will appear small. Rather than plotting the τ_{closed} vs. $1/[Ca]_i$ as was done by Moczydlowski and Latorre (1983, Fig. 7), in Fig. 7 *A* we have plotted the macroscopic activation rate constant, r ($1/\tau_{activation}$) vs. $[Ca]_i$. At high $[Ca]_i$ and moderate to high voltages this parameter approximates $1/\tau_{closed}$. Plotted in this way voltage-dependent changes in the channel's opening rate constant at saturating $[Ca]_i$ are more easily seen. Between +20 and +120 mV, r_{max} varied between 1,000 and 5,000 s^{-1}. This corresponds to a variation in τ_{closed} of from 1 to 0.2 ms. In the plot of Moczydlowski and Latorre (1983, Fig. 7), this variation would be very hard to discern from random variability in the data, and the minimum τ_{closed} might easily be considered to be the same for each voltage. However, upon closer inspection of this plot it appears that each curve does not intersect the τ_{closed} axis at exactly the same point. In fact, there is an increase in the τ_{closed} intercept as the membrane voltage is made more negative. This is expected for a kinetic system whose closed to open rate constant increases with depolarization. It seems unlikely therefore that there is a fundamental difference between the voltage-dependent gating mechanisms of the channels in the two studies, and more likely that methodological differences allowed for intrinsic voltage dependence to be more clearly seen in our study.

A Concerted Step between Closed and Open

A striking feature of macroscopic *mslo* currents is that the time course of both activation and deactivation can be well described by a single exponential function after the first ~100 μs. This was found to be the case under all conditions in which the relaxation time course was accurately determined despite the fact that Ca^{2+} and voltage had strong effects on the time course of *mslo* current relaxation. These results are perhaps surprising given that at least eight kinetic states are necessary to describe the stationary gating behavior of single skeletal muscle BK channels (McManus and Magleby, 1988; 1991), and they suggest that in the gating of the *mslo* channel there is a single conformational change which is rate limiting over a wide range of stimuli. The observation that the time course of *mslo* current activation is still voltage dependent at saturating $[Ca]_i$ argues that the rate limiting conformational change is voltage dependent. Further supporting this idea the *mslo* G-V relation can be fairly well described by a Boltzmann function over a wide range of $[Ca]_i$ as is expected for a system which contains a single voltage dependent step between closed and open, and when estimates of the charge

Published May 1, 1997

associated with forward and backward rate limiting steps at each $[Ca]_i$ are summed, they are similar to equivalent gating charge estimates obtained by fitting the G-V relation with a Boltzmann function (see Tables I and II). Taken together these results suggest that it may be reasonable to model the gating of the *mslo* channel as a single voltage-dependent conformational change between closed and open states with Ca^{2+} binding shifting this equilibrium towards open.

Several observations, however, suggest that this view may be too simple. Single channel records from both native and cloned channels display complex kinetic behavior (Moczydlowski and Latorre, 1983; Pallotta, 1983; McManus and Magleby, 1988; 1991; DiChiara and Reinhart, 1995; Giangiacomo et al., 1995). Gating current studies indicate that there is a component of gating charge which moves very rapidly before *slo* channels open (Horrigan et al., 1996; Ottalia et al., 1996). Also, we and others (Ottalia et al., 1996) have observed a brief delay before the exponentially rising phase of *mslo* current activation. Although this delay lasted typically only ~100 μs and was not studied in depth, it did appear to persist over a wide range of $[Ca]_i$ and membrane potentials. The delay was evident even at ~0.5 nM $[Ca]_i$ where the channels were activating without binding Ca^{2+}. Ca^{2+} binding kinetics therefore cannot explain the delay. To account for this delay we must suppose that there are at least two kinetic steps between closed and open. The presence of more than one step between closed and open is also suggested by the observation that while the *mslo* G-V relation appears fairly well fitted by a simple Boltzmann function, it is often as well or better fitted with a Boltzmann function raised to a power between 1 and 3 (Fig. 14). A sequential scheme with a single voltage-dependent transition along the path from closed to open predicts a G-V relation which takes the form of a Boltzmann function. If there are multiple voltage-dependent steps along this path, the exact shape of the G-V relation will depend on the equilibrium constants of all transitions and the magnitude of the associated gating charges. In general, multiple appreciably voltage-dependent elementary steps lead to G-V relations that deviate from simple Boltzmann behavior, producing a curve whose maximum slope is more shallow than would be observed if all of the gating charge was associated with a single conformational change. For many schemes, the G-V relation can be better approximated by a Boltzmann function raised to a power greater than 1 (Zagotta et al., 1994*b*). That the *mslo* G-V relation can often be better fitted by a Boltzmann function raised to a power greater than 1 suggests that more than one voltage-dependent step exists between closed and open states. Nevertheless, the essentially exponential kinetic behavior of the *mslo* channel coupled with fairly good single Boltzmann fits

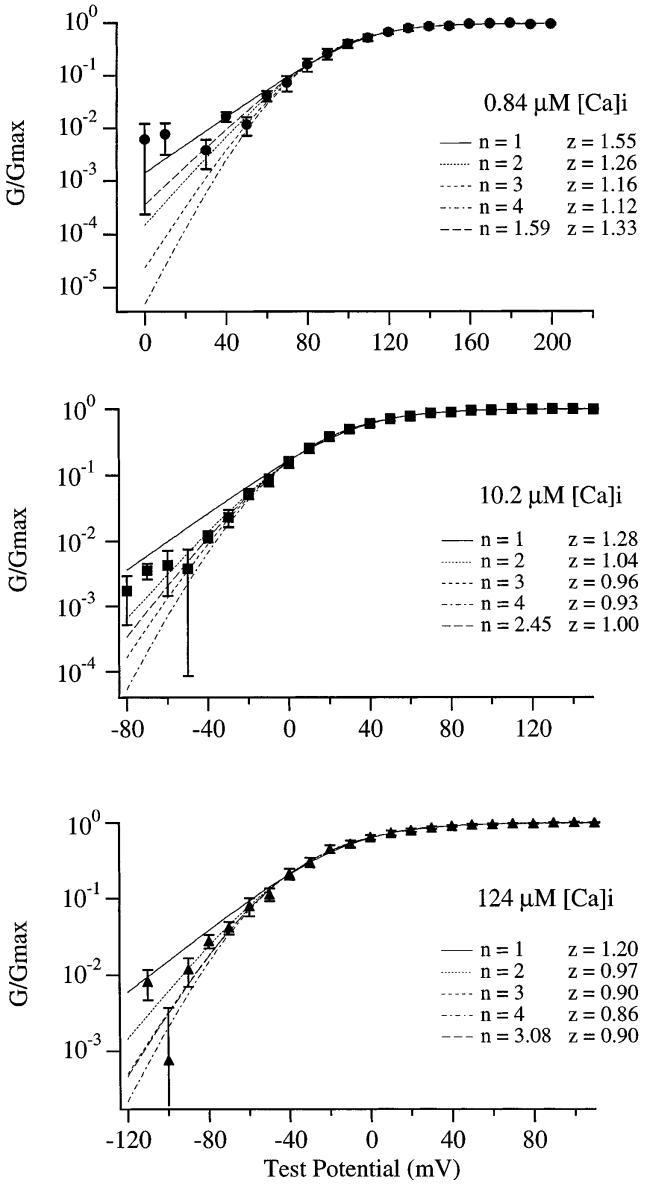

FIGURE 14. *mslo* G-V relations fitted with Boltzmann functions raised to powers between 1 and 4. Displayed are semi-log plots of the *mslo* G-V relation determined with 0.84 (*A*), 10.2 (*B*), and 124 (*C*) μM $[Ca]_i$. Each data set represents the mean of from 5 to 8 experiments. These data are the same as that displayed in Fig. 5 *B*. Each curve has been fitted with the function $G/G_{max} = A[1/(1+e^{-(V-V_{1/2})zF/RT})]^n$. Curves corresponding to the best fit with n = 1, 2, 3, and 4 have been superimposed on the data. For each $[Ca]_i$ a fit with n varying freely is also displayed. The line type indicating n, as well as the fit parameter z, are as indicated on the figure.

to its G-V relation suggests that even if there are multiple conformational changes involved in activation, there must be a high degree of cooperativity between them such that the probability of the channel existing in an intermediate closed state at equilibrium is low. Putting this discussion in more physical terms, if each

Published May 1, 1997

subunit of the tetramer has a voltage-sensing element, then the observations discussed above suggest that these voltage-sensing elements are not acting independently, but rather the movement of one voltage sensor facilitates the movements of others such that together these elements move in a highly concerted manner. This mechanism differs from that of the *shaker* K^+ channel whose voltage sensing elements appear to move independently (Zagotta et al., 1994*a*). Based on our results a high degree of cooperativity between subunits in *mslo* channel opening seems inescapable.

It should be noted that while we have expressed a single species of *mslo* RNA, through some process, such as posttranslational modification, the *mslo* channel populations we have studied may not have been completely homogeneous. This could also give rise to deviation from exponential kinetic behavior, as well as simple Boltzmann steady-state behavior.

mslo Has Less Gating Charge than a Shaker Channel

Boltzmann fits to *mslo* G-V curves over a range of $[Ca]_i$ yielded equivalent gating charge estimates of between 1.1 and 1.9 *e*. At very low $[Ca]_i$, this estimate was somewhat reduced ($\sim$0.8 *e*). Other studies on both native (Barrett et al., 1982; Latorre et al., 1982; Methfessel and Boheim, 1982; Oberhauser et al., 1988) and cloned (Wei and Salkoff, 1986; Butler et al., 1993; Perez et al., 1994; Tseng-Crank et al., 1994; DiChiara and Reinhart, 1995; McCobb et al., 1995; Wallner et al., 1995) channels report values ranging between $\sim$1 and 2 as well. These values suggest that the equivalent gating charge of BK channels may be as much as 12 *e* less than that of the *shaker* channel (Schoppa et al., 1992; Zagotta et al., 1994*b*; Aggarwal and MacKinnon, 1996; Seoh et al., 1996) or DRK1(Kv2.1) (Islas and Sigworth, 1996). However, the fact that the G-V relation for a sequential gating scheme comprised of multiple voltage-dependent steps will be more shallow than it would be if all the gating charge moved in a single step means that fitting a channel's G-V relation with a Boltzmann function will often lead to an underestimate of the true gating charge of the channel. The severity of the underestimate will depend on the number of voltage-dependent steps between closed and open, the extent to which the total gating charge is spread throughout these steps, and the degree of cooperativity of the system. As pointed out by Zagotta et al. (1994*b*), as a gating scheme becomes more concerted such that the equilibrium constant for the last step before opening becomes large relative to early steps, the deviation from simple Boltzmann behavior decreases. In the limit that the relative magnitude of the last step becomes very large, a Boltzmann function which would describe the G-V relation for a two-state system containing all of the gating charge is predicted. This suggests then that for a channel like *mslo*, which appears to have a concerted conformational change between closed and open, Boltzmann fits to the G-V relation may not seriously underestimate the true gating charge of the channel, at least not to the same extent as is seen for the *shaker* channel whose G-V relation deviates more strongly from Boltzmann behavior and whose activation kinetics are much more sigmoid (Zagotta et al., 1994*b*). In the *shaker* channel Boltzmann fitting underestimates the gating charge by a factor of $\sim$3 (Schoppa et al., 1992; Zagotta et al., 1994*b*). Equivalent gating charge estimates of between $\sim$1 and 2 from Boltzmann fits to the *mslo* G-V relation are therefore likely to be no less accurate. Even if these estimates are off by as much as a factor of 3, however, they still indicate that the total gating charge of the *mslo* channel is likely to be no more than 6 *e*, at least $\sim$2-fold less than the best studied purely voltage-gated K^+ channels. Whether the smaller amount of gating charge in the *mslo* channel is due to the fewer basic residues in its S4 region will be important to determine.

A General Scheme for mslo Channel Gating

Despite the arguments above which suggest that it may be better to think of the *mslo* channel as having a highly concerted rather than a single step between closed and open, in considering SCHEME IV we have seen that several properties of *mslo* macroscopic currents can be understood in terms of a kinetic scheme in which there is a central voltage-dependent conformational change both preceded and proceeded by rapid Ca^{2+} binding steps. These properties include: exponential activation and deactivation kinetics, relaxation rates which increase with $[Ca]_i$ at depolarized voltages and decrease with $[Ca]_i$ at hyperpolarized voltages, saturating kinetic behavior at high $[Ca]_i$, and an apparent affinity for Ca^{2+}, as judged by half saturation of the macroscopic activation rate constant, which is much less sensitive to voltage than is the apparent affinity as judged by half saturation of the channels normalized conductance. SCHEME IV, however, cannot account for all aspects of our data as (*a*) it does not allow for channel opening with strong depolarizations in the absence of Ca^{2+} binding, (*b*) it does not predict that membrane voltage can limit the extent to which Ca^{2+} can activate *mslo* channels, and (*c*) it supposes that only two Ca^{2+} molecules bind to the channel. Still, its qualitative success with many aspects of *mslo* gating suggests that its general premise may be worth further consideration.

We can expand SCHEME IV to a form which can qualitatively account for all the properties listed above and yet maintain its essential nature by considering SCHEME V below (the portion of SCHEME V which corresponds to SCHEME IV has been boxed).

Published May 1, 1997

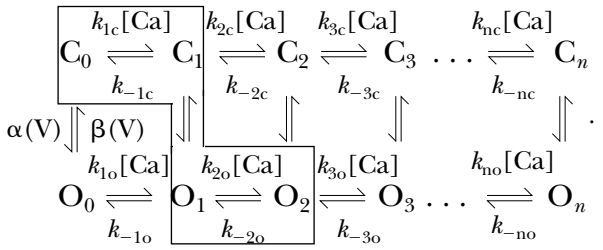

(SCHEME V)

Like SCHEME IV, SCHEME V describes a channel which must undergo a central voltage-dependent conformational change in order to open. Here, however, the channel can open with 0 to n Ca^{2+} molecules bound. In order for this system to be activated by Ca^{2+}, on average, Ca^{2+} must bind more tightly to the open conformation than to the closed. When this is the case the leftward shifting nature of the *mslo* G-V relation with increasing $[Ca]_i$ (Fig. 5) can be understood, because as more Ca^{2+} molecules bind to the channel, the central equilibrium will progressively shift toward opening. It therefore will take less voltage to bring the channel to its maximum open probability. The observation that the $[Ca]_i$ required to half maximally activate *mslo* currents decreases as the membrane voltage is depolarized (Fig. 13 *D*) can also be explained in terms of SCHEME V, as, according to this scheme, it would take fewer bound Ca^{2+} to maximally activate the channel as the membrane voltage is depolarized. In fact, at extremely positive voltages none are required, leading to Ca-independent opening as we have described.

As was the case for SCHEME IV, SCHEME V requires that Ca^{2+} binding is not rate limiting to reproduce the single exponential kinetics observed over a wide range of conditions, and the saturation of the macroscopic activation rate constant at high $[Ca]_i$. It is interesting to consider the possibility more closely, however, that it is the Ca^{2+} binding steps which are rate limiting. If the horizontal rates in SCHEME V were very slow relative to the vertical rates, the channels would move predominately vertically before horizontally, and the activation time course of the population would have many exponential components, at least one for each vertical step in the scheme. If on the other hand the vertical rates were much slower than the horizontal rates, then the channels would redistribute laterally while moving to open, producing relaxation kinetics which would be much more simple. In fact, it can be shown that, in the limit that the Ca^{2+} binding and unbinding rates become very fast relative to the vertical rates such that each horizontal step can be considered to be in a steady state at all times, the kinetics of SCHEME V are described by a single exponential function. The time constant of this exponential will depend on $[Ca]_i$, and on the values of all the vertical rates and horizontal equilibrium constants in the system. Due to the exponential nature of the *mslo* currents, therefore, we favor the idea that it is a Ca^{2+} independent conformational change which is limiting the kinetic behavior of the *mslo* channel over a wide range of conditions.

DiChiara et al. (1995) concluded that it was Ca^{2+} binding which was limiting the activation time course of *dslo* currents in part based on the observation that at high open probabilities the time course of *dslo* macroscopic current activation parallels the cumulative time to first opening of *dslo* single channels and that this time course changes as a function of $[Ca]_i$. This observation, in fact, is not at odds with the above conclusion as, at high open probability and in the rapid Ca^{2+} binding limit, both the time to first opening and the macroscopic activation rate constant of SCHEME V will be determined by the same weighted average of all of the forward rate constants in the system, and the contribution of each rate constant to this average will change as a function of $[Ca]_i$. Their observation that the time course of *dslo* and *hslo* activation is best described by two exponential components, however, may indicate that in these channels Ca^{2+} binding rates are contributing in a more direct way to the kinetics of relaxation than they do for *mslo*.

Wei et al.(1994) have studied the G-V relations of chimeric channels comprised of core (the NH_2 terminus through S8) and tail (after S8 to the COOH terminus) regions from either *mslo* or *dslo* channels. *mslo* has a higher apparent affinity for Ca^{2+} than does *dslo*. Interestingly, they found that when a *dslo* tail was expressed together with a *mslo* core, the *dslo* tail had little effect on the chimeric channel's G-V relation at high $[Ca]_i$ (300 μM). That is, the chimeric channel's G-V relation was very similar to the parent *mslo* channel. At lower $[Ca]_i$ however, much stronger depolarizations were required to activate the chimeric channel as compared to *mslo*. They also found that the reverse chimera's (*dslo-mslo*) G-V relation at high $[Ca]_i$ was in a similar position on the voltage axis to that of the *dslo* channel but was shifted to more hyperpolarized voltages than that of *dslo* at lower $[Ca]_i$. They interpreted these results to indicate that the *slo* channel's Ca^{2+} binding affinity is determined by its tail region, and that the *dslo* tail binds Ca^{2+} with lower affinity than does the *mslo* tail, whereas the channel's closed to open equilibrium at saturating $[Ca]_i$ is determined by its core region.

Some aspects of SCHEME V support this hypothesis. If the *dslo* tail region confers lower Ca^{2+} affinity on the channel than does the *mslo* tail, then, according to SCHEME V, at low [Ca] the chimeric channel's G-V relation would likely lie to the right of the *mslo* G-V relation due to the fact that fewer Ca^{2+} would be bound to the *mslo-dslo* channel. At saturating $[Ca]_i$, however, the two G-V curves would not necessarily be expected to converge. This is because, according to SCHEME V, and in-

Published May 1, 1997

deed for any gating system activated by Ca^{2+}, the position of the G-V relation on the voltage axis at saturating $[Ca]_i$ will not be determined solely by the intrinsic conformational free energy difference between closed and open (in SCHEME V this free energy difference determines the equilibrium constant between C_0 and O_0), but it will also depend on the difference in Ca^{2+} binding energy between closed and open. For SCHEME V the equilibrium constant between closed and open at saturating $[Ca]_i$ is given by

$$K_{sat} = \frac{[O_n]}{[C_n]} = \frac{\alpha(V)}{\beta(V)} \left[\frac{\prod_1^n \left(\frac{k_{-ic}}{k_{ic}} \right)}{\prod_1^n \left(\frac{k_{-io}}{k_{io}} \right)} \right]. \quad (23)$$

The term in square brackets represents the ratio of the product of the Ca^{2+} dissociation constants for Ca^{2+} binding to closed states, to the product of the Ca^{2+} dissociation constants for Ca^{2+} binding to open states. Therefore, changes in Ca^{2+} binding affinities can affect the closed to open equilibrium even at saturating $[Ca]_i$, and changing from *mslo* tail to *dslo* tail might be expected to affect the position of the *mslo-dslo* G-V relation at saturating $[Ca]_i$. Such an effect would not be observed, however, if in changing from *mslo* tail to *dslo* tail, the ratio of Ca^{2+} binding energies between closed and open states remained constant. The observations of Wei et al. therefore suggest that this may be the case. Our results, however, suggest that a more direct way to examine the effects of the core region on the intrinsic conformational energy of the channel would be to examine the G-V relations of the chimeric channels at very low $[Ca]_i$ where the channels are gating without bound Ca^{2+}. If it is the core region that determines the intrinsic energy difference between closed and open, then one would predict that in the zero $[Ca]_i$ limit the *mslo* and *mslo-dslo* G-V relations would again converge. Whether this is actually the case will be interesting to determine.

McManus and Magleby (1991) have considered schemes which take the form of SCHEME V to account for the Ca-dependent, stationary gating properties of skeletal muscle BK channels at +30 mV and have proposed as the simplest model to account for their data a subset of this system shown below.

$$\begin{array}{ccccccc} & k_{1c}[Ca] & & k_{2c}[Ca] & & k_{3c}[Ca] & & k_{4c}[Ca] & \\ C_0 & \rightleftharpoons & C_1 & \rightleftharpoons & C_2 & \rightleftharpoons & C_3 & \rightleftharpoons & C_4 \\ & k_{-1c} & & k_{-2c} & \Uparrow\Downarrow & k_{-3c} & \Uparrow\Downarrow & k_{-4c} & \Uparrow\Downarrow \\ & & & & k_{3o}[Ca] & & k_{4o}[Ca] & & \\ & & & & O_2 & \rightleftharpoons & O_3 & \rightleftharpoons & O_4 \\ & & & & & k_{-3o} & & k_{-4o} & \end{array} \quad \text{(SCHEME VI)}$$

One obvious difference between SCHEME VI and SCHEME V is the absence of direct opening pathways from C_0 and C_1. However, we do not believe this to be an important discrepancy, because in SCHEME V these transitions would not be favored with $[Ca]_i$ between 1 and 25 μM, and at the moderately depolarized voltage they used. Although it was derived from data on different channels, the general form of their model is clearly quite similar to, and a subset of, SCHEME V. McManus and Magleby, however, did not study the voltage dependence of gating. As an exercise, we wondered whether if by supplying voltage dependence to the vertical transitions of SCHEME VI and using the kinetic parameters defined for +30 mV by McManus and Magleby (cell #1), we could account for the kinetics of macroscopic *mslo* currents. We found that if we let the channels distribute among the closed states at negative potentials and then jumped the voltage to +30 mV, the kinetics of this system were similar to *mslo* at low (0.84 μM) $[Ca]_i$ and high (124 μM) $[Ca]_i$. At intermediate $[Ca]_i$, however, the model was either significantly slower (1.7, 4.5 μM $[Ca]_i$) or faster (10.2 μM $[Ca]_i$) than the *mslo* currents, and more than one kinetic component was usually evident. If we assigned to the McManus and Magleby model an amount of gating charge similar to that estimated for *mslo* ($qf = 0.7$, $qb = -0.7$), over a range of voltages, the modified McManus and Magleby model in general showed much slower activation kinetics than *mslo* at $[Ca]_i$ below 124 μM and much faster deactivation kinetics at negative potentials. This result is not surprising as we have studied the α subunit of a cloned channel in a heterologous expression system, while their experiments were done with native skeletal muscle BK channels which may have been composed of α and β subunits. It does indicate, however, that we can not co-opt this system as it stands to account quantitatively for the macroscopic kinetics of the *mslo* channel. The type of detailed studies done by McManus and Magleby certainly must be applied to *mslo* channels. In the broader sense, however, that both detailed single channel analysis and macroscopic current measurements are pointing to a channel with a concerted closed to open conformational changed regulated by multiple Ca^{2+} binding sites lends further credence to the idea that this general view is correct.

We gratefully acknowledge Larry Salkoff for providing the *mslo* clone, Marcus Hoth and Richard Lewis for performing Ca^{2+} concentration measurements by fluorescence microscopy, Victor Corvalan for algorithms for Ca^{2+} concentration calculations, and Frank Horrigan for helpful comments on the manuscript.

This work was supported by a National Institute of Mental Health Silvio Conte Center for Neuroscience Research grant (MH 48108). J. Cui was supported by a postdoctoral fellowship from the Muscular Dystrophy Association. R.W. Aldrich is an investigator with the Howard Hughes Medical Institute.

Original version received 7 October 1996 and accepted version received 27 February 1997.

REFERENCES

Adair, G.S. 1925. The hemoglobin system. VI. The oxygen dissociation curve of hemoglobin. *J. Biol. Chem.* 63:529–545.

Adelman, J.P., K.Z. Shen, M.P. Kavanaugh, R.A. Warren, Y.N. Wu, A. Lagrutta, C.T. Bond, and R.A. North. 1992. Calcium-activated potassium channels expressed from cloned complementary DNAs. *Neuron.* 9:209–216.

Aggarwal, S.K., and R. MacKinnon. 1996. Contribution of the S4 segment to gating charge in the *shaker* K^+ channel. *Neuron.* 16: 1169–1177.

Art, J.J., Y.C. Wu, and R. Fettiplace. 1995. The calcium-activated potassium channels of turtle hair cells. *J. Gen. Physiol.* 105:49–72.

Atkinson, N.S., G.A. Robertson, and B. Ganetzky. 1991. A component of calcium-activated potassium channels encoded by the Drosophila *slo* locus. *Science (Wash. DC).* 253:551–555.

Barrett, J.N., K.L. Magleby, and B.S. Pallotta. 1982. Properties of single calcium-activated potassium channels in cultured rat muscle. *J. Physiol. (Lond.).* 331:211–230.

Blair, L.A., and V.E. Dionne. 1985. Developmental acquisition of Ca^{2+}-sensitivity by K^+ channels in spinal neurones. *Nature (Lond.).* 315:329–331.

Butler, A., S. Tsunoda, D.P. McCobb, A. Wei, and L. Salkoff. 1993. mSlo, a complex mouse gene encoding "maxi" calcium-activated potassium channels. *Science (Wash. DC).* 261:221–224.

Chandler, W.K., A.L. Hodgkin, and H. Meves. 1965. The effect of changing the internal solution on sodium inactivation and related phenomena in giant axons. *J. Physiol. (Lond.).* 180:821–836.

Cornejo, M., S.E. Guggino, and W.B. Guggino. 1987. Modification of Ca^{2+}-activated K^+ channels in cultured medullary thick ascending limb cells by N-bromoacetamide. *J. Membr. Biol.* 99:147–155.

Cox, D.H., J. Cui, and R.W. Aldrich. 1997. Separation of gating properties from permeation and block in *mslo* large conductance Ca-activated K^+ channels. *J. Gen. Physiol.* 109:633–646.

Diaz, F., M. Wallner, E. Stefani, L. Toro, and R. Latorre. 1996. Interaction of internal Ba^{2+} with a cloned Ca^{2+}-dependent K^+ (hslo) channel from smooth muscle. *J. Gen. Physiol.* 107:399–407.

DiChiara, T.J., and P.H. Reinhart. 1995. Distinct effects of Ca^{2+} and voltage on the activation and deactivation of cloned Ca^{2+}-activated K^+ channels. *J. Physiol. (Lond.).* 489:403–418.

Fabiato, A., and F. Fabiato. 1979. Calculator programs for computing the composition of the solutions containing multiple metals and ligands used for experiments in skinned muscle cells. *J. Physiol. (Paris).* 75:463–505.

Findlay, I., M.J. Dunne, and O.H. Petersen. 1985. High-conductance K^+ channel in pancreatic islet cells can be activated and inactivated by internal calcium. *J. Membr. Biol.* 83:169–175.

Frankenhaeuser, B., and A.L. Hodgkin. 1957. The action of calcium on the electrical properties of squid axons. *J. Physiol. (Lond.).* 137:218–244.

Getzoff, E.D., D.E. Cabelli, C.L. Fisher, H.E. Parge, M.S. Viezzoli, L. Banci, and R.A. Hallewell. 1992. Faster superoxide dismutase mutants designed by enhancing electrostatic guidance. *Nature (Lond.).* 358:347–351.

Giangiacomo, K.M., M. Garciacalvo, H.G. Knaus, T.J. Mullmann, M.L. Garcia, and O. McManus. 1995. Functional reconstitution of the large-conductance, calcium-activated potassium channel purified from bovine aortic smooth muscle. *Biochemistry.* 34: 15849–15862.

Golowasch, J., A. Kirkwood, and C. Miller. 1986. Allosteric effects of Mg^{2+} on the gating of Ca^{2+}-activated K^+ channels from mammalian skeletal muscle. *J. Exp. Biol.* 124:5–13.

Grissmer, S., A.N. Nguyen, J. Aiyar, D.C. Hanson, R.J. Mather, G.A. Gutman, M.J. Karmilowicz, D.D. Auperin, and K.G. Chandy. 1994. Pharmacological characterization of five cloned voltage-gated K^+ channels, types Kv1.1, 1.2, 1.3, 1.5, and 3.1, stably expressed in mammalian cell lines. *Mol. Pharmacol.* 45:1227–1234.

Heginbotham, L., T. Abramson, and R. MacKinnon. 1992. A functional connection between the pores of distantly related ion channels as revealed by mutant K^+ channels. *Science (Wash. DC).* 258:1152–1155.

Heginbotham, L., Z. Lu, T. Abramson, and R. MacKinnon. 1994. Mutations in the K^+ channel signature sequence. *Biophys. J.* 66: 1061–1067.

Hill, A.V. 1910. The possible effects of the aggregation of the molecules of hemoglobin on the dissociation curves. *J. Physiol. (Lond.).* 40:iv–vii.

Hille, B. 1992. Ionic Channels of Excitable Membranes, 2nd ed. Sinauer Associates, Inc. Sunderland, MA. pp. 607.

Hille, B., A.M. Woodhull, and B.I. Shapiro. 1975. Negative surface charge near sodium channels of nerve: divalent ions, monovalent ions, and pH. *Philos. Trans. R. Soc. Lond. B Biol. Sci.* 270:301–318.

Horrigan, F.H., J. Cui, D.H. Cox, and R.W. Aldrich. 1996. Gating charge movement from *mslo* Ca^{2+}-activated K^+ channel measured via admittance analysis. *Biophys. J.* 70:A233. (Abstr.).

Hudspeth, A.J., and R.S. Lewis. 1988*a*. Kinetic analysis of voltage- and ion-dependent conductances in saccular hair cells of the bull-frog, Rana catesbeiana. *J. Physiol. (Lond.).* 400:237–274.

Hudspeth, A.J., and R.S. Lewis. 1988*b*. A model for electrical resonance and frequency tuning in saccular hair cells of the bull-frog, Rana catesbeiana. *J. Physiol. (Lond.).* 400:275–297.

Islas, L.D., and F.J. Sigworth. 1996. The limiting slope of Kv2.1 channels shows a gating charge of about $12e_o$. *Biophys. J.* 70:A190. (Abstr.).

Karpen, J.W., A.L. Zimmerman, L. Stryer, and D.A. Baylor. 1988. Gating kinetics of the cyclic-GMP-activated channel of retinal rods: flash photolysis and voltage-jump studies. *Proc. Natl. Acad. Sci. USA.* 85:1287–1291.

Kaupp, U.B., T. Niidome, T. Tanabe, S. Terada, W. Bonigk, W. Stuhmer, N.J. Cook, K. Kangawa, H. Matsuo, T. Hirose, et al. 1989. Primary structure and functional expression from complementary DNA of the rod photoreceptor cyclic GMP-gated channel. *Nature (Lond.).* 342:762–766.

Lagrutta, A., K.Z. Shen, R.A. North, and J.P. Adelman. 1994. Functional differences among alternatively spliced variants of Slowpoke, a Drosophila calcium-activated potassium channel. *J. Biol. Chem.* 269:20347–20351.

Larsson, H.P., O.S. Baker, D.S. Dhillon, and E.Y. Isacoff. 1996. Transmembrane movement of the *shaker* K^+ channel S4. *Neuron.* 16:387–397.

Latorre, R., A. Oberhauser, P. Labarca, and O. Alvarez. 1989. Varieties of calcium-activated potassium channels. *Annu. Rev. Physiol.* 51:385–399.

Latorre, R., C. Vergara, and C. Hidalgo. 1982. Reconstitution in planar lipid bilayers of a Ca^{2+}-dependent K^+ channel from transverse tubule membranes isolated from rabbit skeletal muscle. *Proc. Natl. Acad. Sci. USA.* 79:805–809.

Liman, E.R., P. Hess, F. Weaver, and G. Koren. 1991. Voltage-sensing residues in the S4 region of a mammalian K^+ channel. *Nature (Lond.).* 353:752–756.

Logothetis, D.E., B.F. Kammen, K. Lindpaintner, D. Bisbas, and G.B. Nadal. 1993. Gating charge differences between two voltage-gated K^+ channels are due to the specific charge content of their respective S4 regions. *Neuron.* 10:1121–1129.

Lopez, G.A., Y.N. Jan, and L.Y. Jan. 1991. Hydrophobic substitution mutations in the S4 sequence alter voltage-dependent gating in Shaker K^+ channels. *Neuron.* 7:327–336.

Lux, H.D., E. Neher, and A. Marty. 1981. Single channel activity associated with the calcium dependent outward current in Helix pomatia. *Pflüg. Arch.* 389:293–295.

MacKinnon, R., and G. Yellen. 1990. Mutations affecting TEA blockade and ion permeation in voltage-activated K^+ channels. *Science (Wash. DC).* 250:276–279.

Mannuzzu, L.M., M.M. Moronne, and E.Y. Isacoff. 1996. Direct physical measure of conformational rearrangement underlying potassium channel gating. *Science (Wash. DC).* 271:213–216.

Markwardt, F., and G. Isenberg. 1992. Gating of maxi K^+ channels studied by Ca^{2+} concentration jumps in excised inside-out multichannel patches (myocytes from guinea pig urinary bladder). *J. Gen. Physiol.* 99:841–862.

Marty, A. 1981. Ca-dependent K channels with large unitary conductance in chromaffin cell membranes. *Nature (Lond.).* 291: 497–500.

Marty, A. 1989. The physiological role of calcium-dependent channels. *Trends Neurosci.* 12:420–424.

McCobb, D.P., N.L. Fowler, T. Featherstone, C.J. Lingle, M. Saito, J.E. Krause, and L. Salkoff. 1995. A human calcium-activated potassium channel gene expressed in vascular smooth muscle. *Am. J. Physiol.* 269:H767–H777.

McManus, O.B. 1991. Calcium-activated potassium channels: regulation by calcium. *J. Bioenerg. Biomembr.* 23:537–560.

McManus, O.B., A.L. Blatz, and K.L. Magleby. 1985. Inverse relationship of the durations of adjacent open and shut intervals for Cl and K channels. *Nature (Lond.).* 317:625–627.

McManus, O.B., L.M. Helms, L. Pallanck, B. Ganetzky, R. Swanson, and R.J. Leonard. 1995. Functional role of the beta subunit of high conductance calcium-activated potassium channels. *Neuron.* 14:645–650.

McManus, O.B., and K.L. Magleby. 1988. Kinetic states and modes of single large-conductance calcium-activated potassium channels in cultured rat skeletal muscle. *J. Physiol. (Lond.).* 402:79–120.

McManus, O.B., and K.L. Magleby. 1991. Accounting for the Ca(2+)-dependent kinetics of single large-conductance Ca(2+)-activated K^+ channels in rat skeletal muscle. *J. Physiol. (Lond.).* 443:739–777.

Meera, P., M. Wallner, Z. Jiang, and L. Toro. 1996. A calcium switch for the functional coupling between alpha (hslo) and beta subunits (KV,Ca beta) of maxi K channels. *FEBS Lett.* 382:84–88.

Methfessel, C., and G. Boheim. 1982. The gating of single calcium-dependent potassium channels is described by an activation/blockade mechanism. *Biophys. Struct. Mech.* 9:35–60.

Moczydlowski, E., and R. Latorre. 1983. Gating kinetics of Ca^{2+}-activated K^+ channels from rat muscle incorporated into planar lipid bilayers. Evidence for two voltage-dependent Ca^{2+} binding reactions. *J. Gen. Physiol.* 82:511–542.

Neyton, J. 1996. A Ba^{2+} chelator suppresses long shut events in fully activated high-conductance Ca^{2+}-dependent K^+ channels. *Biophys. J.* 71:220–226.

Oberhauser, A., O. Alvarez, and R. Latorre. 1988. Activation by divalent cations of a Ca^{2+}-activated K^+ channel from skeletal muscle membrane. *J. Gen. Physiol.* 92:67–86.

Ottalia, M., F. Noceti, R. Olcese, M. Wallner, R. Lattore, E. Stefani, and L. Toro. 1996. Charge movement in a voltage and Ca^{2+} sensitive potassium channel (*hslo*). *Biophys. J.* 70:A193. (Abstr.).

Pak, M.D., M. Covarrubias, A. Ratcliffe, and L. Salkoff. 1991. A mouse brain homolog of the Drosophila Shab K^+ channel with conserved delayed-rectifier properties. *J. Neurosci.* 11:869–880.

Pallotta, B.S. 1983. Single channel recordings from calcium-activated potassium channels in cultured rat muscle. *Cell Calcium.* 4: 359–370.

Pallotta, B.S. 1985*a*. Calcium-activated potassium channels in rat muscle inactivate from a short-duration open state. *J. Physiol. (Lond.).* 363:501–516.

Pallotta, B.S. 1985b. N-bromoacetamide removes a calcium-dependent component of channel opening from calcium-activated potassium channels in rat skeletal muscle. *J. Gen. Physiol.* 86:601–611.

Pallotta, B.S., K.L. Magleby, and J.N. Barrett. 1981. Single channel recordings of Ca^{2+}-activated K^+ currents in rat muscle cell culture. *Nature (Lond.).* 293:471–474.

Papazian, D.M., L.C. Timpe, Y.N. Jan, and L.Y. Jan. 1991. Alteration of voltage-dependence of Shaker potassium channel by mutations in the S4 sequence. *Nature (Lond.).* 349:305–310.

Perez, G., A. Lagrutta, J.P. Adelman, and L. Toro. 1994. Reconstitution of expressed KCa channels from Xenopus oocytes to lipid bilayers. *Biophys. J.* 66:1022–1027.

Perozo, E., T.L. Santacruz, E. Stefani, F. Bezanilla, and D.M. Papazian. 1994. S4 mutations alter gating currents of Shaker K channels. *Biophys. J.* 66:345–354.

Pilling, M.J., and P.W. Seakins. 1995. Reaction Kinetics. Oxford University Press. New York.

Salomao, L., G. Wark, W.P. Dubinsky, and S.G. Schultz. 1992. Effect of trypsin on a Ca(2+)-activated K^+ channel reconstituted into planar phospholipid bilayers. *Am. J. Physiol.* 262:C971–C974.

Schoppa, N.E., K. McCormack, M.A. Tanouye, and F.J. Sigworth. 1992. The size of gating charge in wild-type and mutant Shaker potassium channels. *Science (Wash. DC).* 255:1712–1715.

Seoh, S., D. Sigg, D.M. Papazian, and F. Bezanilla. 1996. Voltage-sensing residues in the S2 and S4 segments of the *shaker* K^+ channel. *Neuron.* 16:1159–1167.

Shen, K.Z., A. Lagrutta, N.W. Davies, N.B. Standen, J.P. Adelman, and R.A. North. 1994. Tetraethylammonium block of Slowpoke calcium-activated potassium channels expressed in Xenopus oocytes: evidence for tetrameric channel formation. *Pflüg. Arch.* 426:440–445.

Sigworth, F.J. 1994. Voltage gating of ion channels. *Q. Rev. Biophys.* 27:1–40.

Singer, J.J., and J.J. Walsh. 1987. Characterization of calcium-activated potassium channels in single smooth muscle cells using the patch-clamp technique. *Pflüg. Arch.* 408:98–111.

Smith-Maxwell, C.J., R.A. Taylor, and R.W. Aldrich. 1994. Amino acids responsible for slowing activation in *shaker* potassium channel mutants. *Soc. Neurosci. Abstr.* 20:863.

Smoluchowski, M.V. 1916. Drei vortrage uber diffusion, broensche molekularbewegung und koagulation von kolloidteilchen. *Phys. Z.* 17:557–571; 585–599.

Stevens, C.F. 1978. Interactions between intrinsic membrane pro-

tein and electric field. An approach to studying nerve excitability. *Biophys. J.* 22:295–306.

Stuhmer, W., F. Conti, H. Suzuki, X.D. Wang, M. Noda, N. Yahagi, H. Kubo, and S. Numa. 1989. Structural parts involved in activation and inactivation of the sodium channel. *Nature (Lond.).* 339: 597–603.

Tseng-Crank, J., C.D. Foster, J.D. Krause, R. Mertz, N. Godinot, T.J. DiChiara, and P.H. Reinhart. 1994. Cloning, expression, and distribution of functionally distinct Ca(2+)-activated K^+ channel isoforms from human brain. *Neuron.* 13:1315–1330.

Wallner, M., P. Meera, M. Ottolia, R. Kaczorowski, R. Latorre, M.L. Garcia, E. Stefani, and L. Toro. 1995. Characterization of and modulation by a β-Subunit of a human maxi K_{Ca} channel cloned from myometrium. *Receptors and Channels.* 3:185–199.

Wallner, M., P. Meera, and L. Toro. 1996. Determinant for beta-subunit regulation in high-conductance voltage-activated and Ca(2+)-sensitive K^+ channels: an additional transmembrane region at the N terminus. *Proc. Natl. Acad. Sci. USA.* 93:14922–14927.

Wei, A., and L. Salkoff. 1986. Occult Drosophila calcium channels and twinning of calcium and voltage-activated potassium channels. *Science (Wash. DC).* 233:780–782.

Wei, A., C. Solaro, C. Lingle, and L. Salkoff. 1994. Calcium sensitivity of BK-type K_{Ca} channels determined by a separable domain. *Neuron.* 13:671–681.

Wong, B.S., H. Lecar, and M. Adler. 1982. Single calcium-dependent potassium channels in clonal anterior pituitary cells. *Biophys. J.* 39:313–317.

Woodhull, A.M. 1973. Ionic blockage of sodium channels in nerve. *J. Gen. Physiol.* 61:687–708.

Wu, Y.C., J.J. Art, M.B. Goodman, and R. Fettiplace. 1995. A kinetic description of the calcium-activated potassium channel and its application to electrical tuning of hair cells. *Prog. Biophys. Mol. Biol.* 63:131–158.

Yang, N., A.J. George, and R. Horn. 1996. Molecular basis of charge movement in voltage-gated sodium channels. *Neuron.* 16:113–122.

Yang, N., and R. Horn. 1995. Evidence for voltage-dependent S4 movement in sodium channels. *Neuron.* 15:213–218.

Yellen, G., M.E. Jurman, T. Abramson, and R. MacKinnon. 1991. Mutations affecting internal TEA blockade identify the probable pore-forming region of a K^+ channel. *Science (Wash. DC).* 251: 939–942.

Yool, A.J., and T.L. Schwarz. 1991. Alteration of the ionic selectivity of a K channel by mutation of the H5 region. *Nature (Lond.).* 349: 700–704.

Zagotta, W.N., T. Hoshi, and R.W. Aldrich. 1994*a.* Shaker potassium channel gating. III. Evaluation of kinetic models for activation. *J. Gen. Physiol.* 103:321–362.

Zagotta, W.N., T. Hoshi, J. Dittman, and R.W. Aldrich. 1994*b.* Shaker potassium channel gating. II. Transitions in the activation pathway. *J. Gen. Physiol.* 103:279–319.